

MIT OpenCourseWare

<http://ocw.mit.edu>

*Electromechanical Dynamics*

For any use or distribution of this textbook, please cite as follows:

Woodson, Herbert H., and James R. Melcher. *Electromechanical Dynamics*. 3 vols. (Massachusetts Institute of Technology: MIT OpenCourseWare). <http://ocw.mit.edu> (accessed MM DD, YYYY). License: Creative Commons Attribution-NonCommercial-Share Alike

For more information about citing these materials or our Terms of Use, visit: <http://ocw.mit.edu/terms>

## Chapter 7

# MAGNETIC DIFFUSION AND CHARGE RELAXATION

### 7.0 INTRODUCTION

There are two important reasons for introducing a distributed or continuum description of electromechanical interactions. The most obvious is that the mechanical system may be an elastic or fluid medium, with the electric or magnetic force distributed throughout. In this case the electrical and mechanical equations of motion are likely to have both time and space coordinates as independent variables. As we shall see in later chapters, there is a need for this model when the dynamical times of interest (say the period of a sinusoidal excitation) are on the same order as the time required for a disturbance to propagate from one extreme to another in the mechanical system.\*

The second reason for introducing a continuum model concerns characteristic times that arise because of competing energy storage and dissipation mechanisms in the electrical system; for example, a lumped inductance  $L$ , shunted by a resistance  $R$ , constitutes a simple magnetic field system. In the absence of motion (which could change the inductance  $L$ ) this circuit has a time constant  $L/R$ . The response of the circuit to an excitation depends greatly on the time constant (or period) of the excitation relative to  $L/R$ . Similarly, the behavior of magnetic field systems involving conducting materials depends considerably on the relative values of times associated with the motion or with electrical excitation and times that characterize the competing energy storage and dissipation phenomena. This point can best be made in terms of a simple example.

\* Note that we neglected similar electromagnetic propagational effects starting in Chapter 1, when the quasi-static electric and magnetic field systems were introduced. This is an extremely good approximation in most systems because the velocity of light is usually much greater than any velocity of propagation for a mechanical or an electromechanical disturbance.

Figure 7.0.1 shows what can be thought of as a one-turn inductor (the perfectly conducting plates short-circuited at the end by a perfectly conducting plate) shunted by a resistance (the block with a conductivity  $\sigma$ ). Suppose that the plates are excited at the left end by a sinusoidally varying current source with the frequency  $\omega$ . At very low frequencies (essentially direct current) we know that this current will flow through the perfectly conducting end plate. As the frequency is raised, however, the rate of change of the time-varying magnetic field will induce a voltage across the block and a current will flow through it between the top and bottom plates. In terms of lumped-parameter models, we could determine this current by attributing a resistance to the block. The block itself, however, has finite dimensions, and we could think of breaking it into two sections and modeling each section by

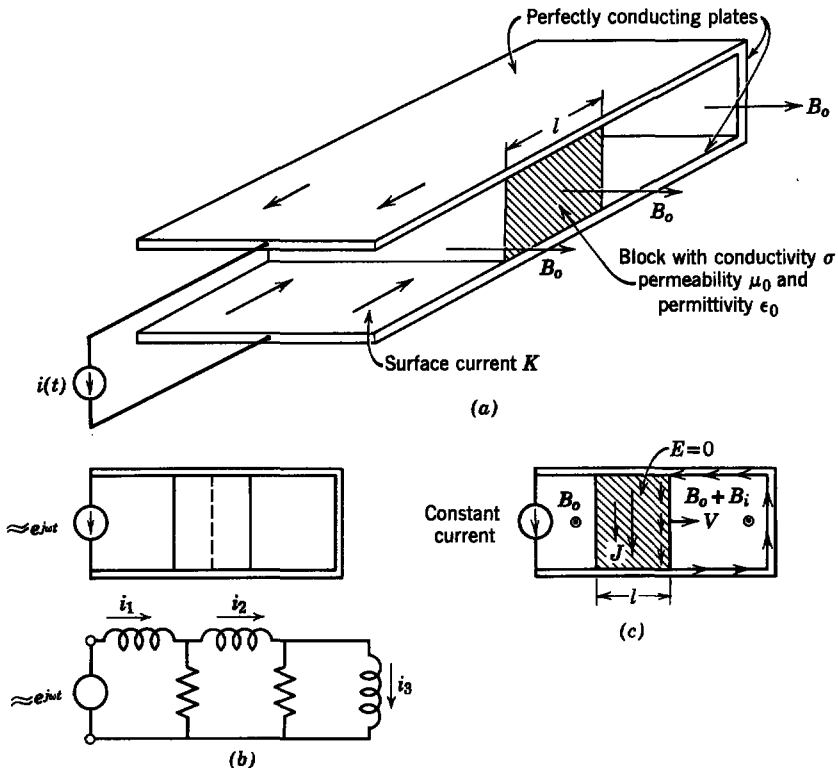


**Fig. 7.0.1** (a) A pair of perfectly conducting plates short-circuited at one end by a perfectly conducting plate and driven at the other end by a current source: a block of conductivity  $\sigma$  makes electrical contact between the plates as shown; (b) equivalent circuit that shows the effect of magnetic diffusion on the currents induced in the block when the source is time-varying; (c) block moving with a velocity  $V$  induces currents that can alter the imposed magnetic field significantly.

a resistance. We now have the equivalent circuit shown in Fig. 7.0.1*b*, in which it is easy to see that at very low frequencies  $i_1 = i_2 = i_3$ . As the frequency is raised, the reactances become significant and  $i_1 > i_2 > i_3$ . In fact, at very high frequencies we expect that current  $i_3$  will be very small. This simple problem points up why a continuum model is required. If the currents  $i_1$  and  $i_2$  are not equal (i.e., if the current through the block is not uniform) to a degree that depends on the dynamical nature of the excitation, what value of resistance do we use to characterize the block? A similar problem exists in attributing one or more equivalent inductances to the system. Our dilemma is brought about by not knowing where the currents flow or, to put it another way, of not knowing how the magnetic field is distributed in space. In the following sections a knowledge of the distribution of magnetic field is our objective, as we discuss the physical phenomenon of *magnetic diffusion*.

In the situation just discussed the time that determined the appropriate system model was  $2\pi/\omega$ , or the period of excitation. In electromechanical problems the motion is responsible for introducing characteristic times which also play an important role in determining the distribution of magnetic field. This can be illustrated by considering again the system of Fig. 7.0.1, this time with the block moving with the velocity  $V$ , as shown in Fig. 7.0.1*c*, and with constant excitation current.

We might model this system by assuming that the constant magnetic flux density  $B_o$ , induced by the current source, is the only magnetic field everywhere between the plates. Then, because of the perfectly conducting end plate, the electric field  $E$  between the plates would be zero. It follows [from (6.3.5)] (Ohm's law for moving media is  $\mathbf{J}' = \sigma\mathbf{E}'$ , where field transformations (Table 6.1, Appendix E) require that  $\mathbf{E}' = \mathbf{E} + \mathbf{v} \times \mathbf{B}$  and  $\mathbf{J}'_f = \mathbf{J}_f$ .) that the motion induces a current density  $J$  of

$$J = VB_o\sigma. \quad (7.0.1)$$

(Here for purposes of illustration we assume that the plates have sufficient extent to justify plane parallel geometry.) Now, we could use this current, together with the imposed magnetic field  $B_o$ , to compute the magnetic force on the block. In doing so, however, we assume that the magnetic field induced by the current  $J$  is negligible compared with the imposed field  $B_o$ . We can establish when this assumption is valid by computing the addition  $B_i$  to the magnetic flux density to the right of the moving block. Constraints on the problem require that  $J$  flow through the end plate to the right, where there is an addition to the surface current  $K$  of

$$K_i = Jl. \quad (7.0.2)$$

Hence the induced magnetic field in the region to the right is

$$B_i = \mu_0 Jl. \quad (7.0.3)$$

It follows from (7.0.1) and (7.0.3) that the ratio of the induced magnetic field to the imposed magnetic field is

$$\frac{B_i}{B_o} = \mu_0 \sigma V l = R_m. \quad (7.0.4)$$

This dimensionless quantity is called the *magnetic Reynolds number*.<sup>\*</sup> From our example we know that if  $R_m$  is significant compared with unity the magnetic field will be altered appreciably by the motion. Of course, this means that the distribution of current within the block will also be dependent on the motion. From (7.0.4) a block with a large dimension  $l$ , a large velocity  $V$ , or a high conductivity  $\sigma$  will require a continuum model to determine the current distribution. One of our objectives in the sections that follow is to indicate electromechanical models that can be used under various conditions of the excitation and mechanical motion.

In electric field systems we are concerned about the distribution of charge and the associated electric field. Here we can think of a simple system in which a resistance  $R$  is connected in series with a capacitance  $C$ . The time constant is then  $RC$ , and when the period of an excitation is on the order of this time we expect that lumped parameter models may be of dubious significance.

Consider, as an example, the system shown in Fig. 7.0.2. Here, a resistive sheet is placed adjacent to a pair of perfectly conducting electrodes with the potential difference  $v$ . A circuit model for this system is shown in Fig. 7.0.2*b*, where the plates form capacitors with the resistive sheet and the sheet is modeled by a single resistance. A more refined model, also shown in Fig. 7.0.2*b*, divides each of the capacitors into two sections and recognizes that the outermost capacitances are connected to a larger series resistance than the inner capacitances.

It is apparent from this latter model that the distribution of charge among the capacitances (hence on the surface of the sheet) is dependent on the frequency of excitation. At very low frequencies the charge would be evenly distributed among the capacitances. As the frequency is raised, the outside capacitances, which have larger series resistances, will support less charge than the inside capacitances. Thus we are in a dilemma about how the capacitances and resistances should be computed and a continuum model is appropriate.

A case in which material motion can have an effect on the charge distribution is shown in Fig. 7.0.2*c*. Here the resistive sheet moves to the right with the velocity  $V$ . If the motion has a negligible effect on the surface charge,

<sup>\*</sup> See, for example, W. F. Hughes, and F. J. Young, *The Electromagnetodynamics of Fluids*, Wiley, New York (1966), p. 154.

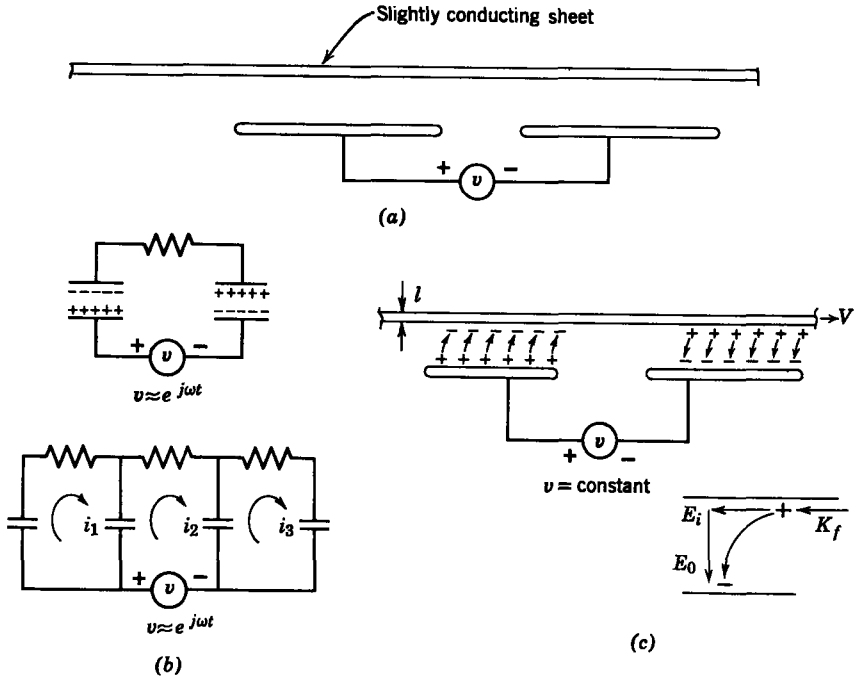


**Fig. 7.0.2** (a) A slightly conducting sheet is placed adjacent to a pair of perfectly conducting plates with the potential difference  $v$ ; (b) equivalent circuit for case in which excitation is sinusoidal: each section of the sheet can be thought of as forming a capacitor with the opposite electrode, but each capacitance has a different series resistance, as shown by the bottom, more refined, circuit; (c) the motion of the sheet, moving with velocity  $V$  and a constant potential difference on the plates, induces a shift in the charge distribution and an electric field  $E_i$ .

the electric field intensity  $E_0$  in the section to the right is related to the surface charge density  $\sigma_f$  by

$$\sigma_f = \epsilon_0 E_0. \tag{7.0.5}$$

We model the resistive material as a sheet having conductivity  $\sigma$ ; hence Ohm's law written in the moving frame of the material requires that  $\mathbf{K}'_f = \sigma l \mathbf{E}'_i$ , where  $l$  is the sheet thickness. Field transformations\* then require  $\mathbf{K}'_f = \mathbf{K}_f - \sigma_f \mathbf{V}$  and  $\mathbf{E}'_i = \mathbf{E}_i$  so that

$$K_f = \sigma l E_i - \sigma_f V. \tag{7.0.6}$$

In the steady state there is no current to the right; hence  $K_f = 0$ . From (7.0.6) there is then an induced electric field intensity given by

$$E_i = \frac{\sigma_f V}{\sigma l}. \tag{7.0.7}$$

\* Table 6.1, Appendix E.

It follows from this expression and (7.0.5) that the ratio of the induced electric field intensity  $E_i$  to the imposed electric field intensity  $E_0$  is

$$\frac{E_i}{E_0} = \frac{\epsilon_0 V}{\sigma l} = R_e \quad (7.0.8)$$

This dimensionless ratio  $R_e$  is called the *electric Reynolds number*.<sup>\*</sup> When this number is significant compared with unity, motion has an appreciable effect on the charge distribution. To understand situations of this kind a continuum model is required.

In the sections that follow we first undertake a study of magnetic field systems (magnetic diffusion) and then electric field systems (charge relaxation). As we have illustrated, our objective is to use a series of examples as vehicles for establishing an understanding of situations in which the distributions of currents and charges are not known until after the problem has been solved.

## 7.1 MAGNETIC FIELD DIFFUSION

In quasi-static magnetic field systems, which consist primarily of magnetizable and conducting materials, magnetic field diffusion is the principal phenomenon that determines what further approximations can be made. Because a general problem is virtually impossible to solve, we will explore diffusion by using a set of simple examples.

To set the stage for studying these examples we first review the mathematical description of a magnetic field system. We assume all materials (magnetizable and/or conducting) to be electrically linear and isotropic. Thus we write the field equations as [see Table 1.2 and (6.3.5.)]†

$$\nabla \times \mathbf{H} = \mathbf{J}_f, \quad (7.1.1)$$

$$\nabla \cdot \mathbf{B} = 0, \quad (7.1.2)$$

$$\mathbf{B} = \mu \mathbf{H}, \quad (7.1.3)$$

$$\nabla \times \mathbf{E} = - \frac{\partial \mathbf{B}}{\partial t}, \quad (7.1.4)$$

$$\mathbf{J}_f = \sigma(\mathbf{E} + \mathbf{v} \times \mathbf{B}). \quad (7.1.5)$$

In these equations the velocity  $\mathbf{v}$  of the conducting material is measured with respect to the inertial coordinate system in which all the field quantities are measured. For our present treatment we assume that the velocity  $\mathbf{v}$  is independently specified as a function of space and time. After we have introduced

<sup>\*</sup> O. M. Stuetzer, "Magnetohydrodynamics and Electrohydrodynamics," *Phys. Fluids*, 5, No. 3, 534-544 (May 1962).

† See Table 1.2, Appendix E, and footnote on p. 332.

continuum mechanics, in later chapters, we shall be prepared to treat situations in which the velocity  $\mathbf{v}$  is a dependent variable.

To illustrate the different phenomena that can occur it is helpful to eliminate all but one variable from (7.1.1) to (7.1.5) and study the resulting expression. For this purpose we assume that the materials are homogeneous (this means that  $\mu$  and  $\sigma$  are not functions of space but that they may be functions of time) and eliminate all variables except the flux density  $\mathbf{B}$ . We use (7.1.5) to eliminate  $\mathbf{E}$  from (7.1.4).

$$\frac{1}{\sigma} \nabla \times \mathbf{J}_f - \nabla \times (\mathbf{v} \times \mathbf{B}) = - \frac{\partial \mathbf{B}}{\partial t}. \quad (7.1.6)$$

Next, we use (7.1.3) to eliminate  $\mathbf{H}$  from (7.1.1):

$$\frac{1}{\mu} \nabla \times \mathbf{B} = \mathbf{J}_f. \quad (7.1.7)$$

The curl of this expression, substituted into (7.1.6), yields

$$\frac{1}{\mu\sigma} \nabla \times (\nabla \times \mathbf{B}) - \nabla \times (\mathbf{v} \times \mathbf{B}) = - \frac{\partial \mathbf{B}}{\partial t}. \quad (7.1.8)$$

We use a vector identity\* and (7.1.2) to rewrite the first term on the left of (7.1.8) and obtain the desired expression involving a single dependent variable, the magnetic flux density  $\mathbf{B}$ :

$$- \frac{1}{\mu\sigma} \nabla^2 \mathbf{B} + \frac{\partial \mathbf{B}}{\partial t} = \nabla \times (\mathbf{v} \times \mathbf{B}). \quad (7.1.9)$$

This equation describes the distribution of magnetic field in the conducting medium.† It includes both the effects of the time-varying magnetic field and the material motion, hence it can be used to analyze the situations shown in Fig. 7.0.1. In a continuum electromechanical problem (7.1.9) plays the same role as the electrical circuit equations played in the lumped-parameter magnetic field systems of the preceding chapters. In fact, there is considerable analogy between (7.1.9) and electrical circuit equations that we encountered in Chapters 3 to 6; for example, the dynamics of a coil in a magnetic field were described in Section 5.1.3 by (5.1.31):

$$-i_1 R - L_1 \frac{di_1}{dt} = AB_o \cos \theta \frac{d\theta}{dt}, \quad (7.1.10)$$

\*  $\nabla \times (\nabla \times \mathbf{B}) = \nabla(\nabla \cdot \mathbf{B}) - \nabla^2 \mathbf{B}$ .

† This equation assumes great importance in the determination of magnetic field origins in the liquid core of the earth. In this context it is sometimes referred to as Bullard's equation. (See T. G. Cowling, *Magnetohydrodynamics*, Interscience, New York, 1957, pp. 4, 77.)

where  $R$  and  $L_1$  are the resistance and inductance of a coil that rotates in the flux density  $B_0$  with the angular displacement  $\theta$ . This expression states that the voltage developed by the motion of the coil in the magnetic field (the "speed voltage" on the right-hand side) is taken up by the voltage drop across the resistance and the inductance of the coil. Similarly, the right-hand side of (7.1.9) is a rate of change of the flux density caused by the motion, and this change is taken up by a flux change due to ohmic dissipation ( $-(1/\mu\sigma)\nabla^2\mathbf{B}$ ) and by a time rate of change of flux density ( $\partial\mathbf{B}/\partial t$ ) at the point.

In the absence of material motion (7.1.9) reduces to the *diffusion equation*.\*

$$\frac{1}{\mu\sigma}\nabla^2\mathbf{B} = \frac{\partial\mathbf{B}}{\partial t}. \quad (7.1.11)$$

This expression is appropriate to the analysis of a problem such as that shown in Fig. 7.0.1*b*, in which the conductor is fixed and the distribution of magnetic field is required. We can think of it as a continuum representation of the dynamics of a distributed system of inductances and resistances. In Section 7.1.1 an example is presented to establish the physical phenomena represented by (7.1.11).

A second limiting case of (7.1.9) of considerable importance results when there is motion but steady-state conditions have been established. Then (7.1.9) reduces to

$$-\frac{1}{\mu\sigma}\nabla^2\mathbf{B} = \nabla \times (\mathbf{v} \times \mathbf{B}). \quad (7.1.12)$$

Here the increase in flux density due to the motion is entirely absorbed by the ohmic dissipation in the material. Physical situations consistent with this limit are considered in Section 7.1.2.

Some of the most important engineering applications involving magnetic diffusion are made possible because there are time-varying excitations in the presence of material motion. The induction machine of Section 4.1.6*b* is an example of an interaction of this type. In general, (7.1.9) is required to analyze these problems, which are exemplified in Sections 7.1.3 and 7.1.4. In fact, the example considered in Section 7.1.4 illustrates the significance of the lumped parameter model for an induction machine.

\* This form of equation is found to describe a variety of dissipative continuum phenomena, including heat conduction, neutron diffusion, and the diffusion of fluid vorticity. See, for example, R. B. Bird, W. E. Stewart, and E. N. Lightfoot, *Transport Phenomena*, Wiley, New York, 1960, p. 352. A. M. Weinberg and E. P. Wigner, *The Physical Theory of Neutron Chain Reactors*, University of Chicago Press, Chicago, 1958, p. 194. H. Schlichting, *Boundary Layer Theory*, McGraw-Hill, New York, 1960, p. 58.

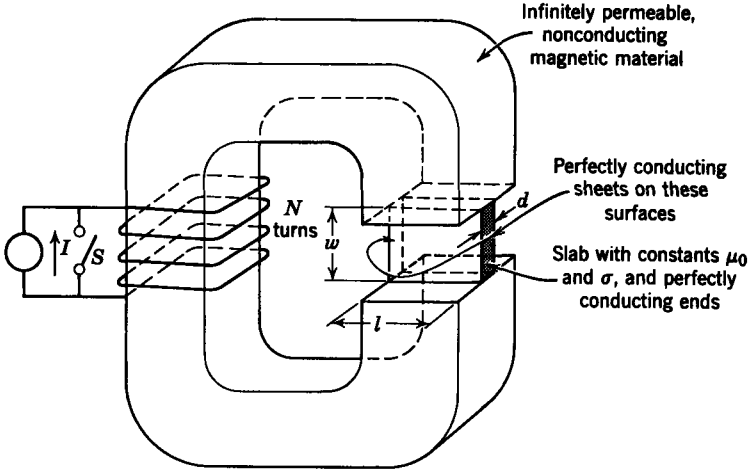


**Fig. 7.1.1** System for studying magnetic diffusion as an electrical transient. A slab of conducting material is placed in the gap of a magnetic circuit excited by a step function of current. An end view of the slab is shown in Fig. 7.1.2.

**7.1.1 Diffusion as an Electrical Transient**

To obtain a firm understanding of the basic electromagnetic phenomena that occur in magnetic field systems we consider first a simple example in which all materials are at rest and we study the diffusion of a magnetic field into (or out of) a rectangular slab of material. The physical situation is shown in Fig. 7.1.1. The system consists of an electromagnet made of

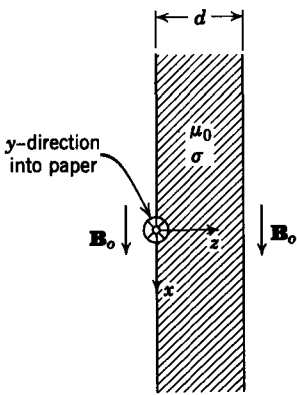


**Fig. 7.1.2** Coordinate system for studying one-dimensional diffusion. At time  $t = 0^+$  the magnetic field is distributed as shown in Fig. 7.1.3.

infinitely permeable, nonconducting magnetic material with an air gap of length  $w$  and excited through the  $N$ -turn winding by a constant-current source  $I$  which can be turned on or off by the switch  $S$ . In the air gap is a slab of non-magnetizable ( $\mu = \mu_0$ ) material of the dimensions shown and with constant electrical conductivity  $\sigma$ .

We assume that the switch  $S$  is initially closed so that there is no current through the winding and no flux in the magnet. At  $t = 0$  switch  $S$  is opened, and we wish to determine the time history of the flux density near the center of the slab. The coordinate system is defined in Fig. 7.1.2. We assume that the slab width  $w$  and length  $l$  are large enough compared with the thickness  $d$  to consider the slab as

infinitely large in the  $x$ - and  $y$ -directions. Moreover, we neglect fringing at the edges of the air gap; consequently, the flux density will have only an  $x$ -component. With switch  $S$  opened at  $t = 0$ , the boundary conditions on the slab are for  $t > 0$ ,  $z < 0$ ,  $z > d$ ,

$$\mathbf{B} = \mathbf{i}_x B_o, \quad (7.1.13)$$

where  $B_o$  (see Section 2.1.1) is given by

$$B_o = \frac{\mu_0 N I}{w}. \quad (7.1.14)$$

In this one-dimensional problem there is only an  $x$ -component of  $\mathbf{B}$  and it varies only with  $z$ ; thus we write the  $x$ -component of (7.1.11) as

$$\frac{1}{\mu_0 \sigma} \frac{\partial^2 B_x}{\partial z^2} = \frac{\partial B_x}{\partial t}. \quad (7.1.15)$$

Within the slab ( $0 < z < d$ ) the flux density is zero immediately after the switch  $S$  is opened

$$\text{at } t = 0^+; \quad B_x = 0. \quad (7.1.16)$$

This condition follows from (7.1.6) with  $\mathbf{v} = 0$ , which we integrate around an arbitrary fixed contour within the conductor. Then by Stokes's theorem we have

$$\frac{1}{\sigma} \oint_C \mathbf{J}_f \cdot d\mathbf{l} = - \frac{\partial}{\partial t} \int_S \mathbf{B} \cdot \mathbf{n} \, da.$$

If  $\mathbf{B}$  has a finite value just after the switch is opened, the time derivative on the right (assuming that the integral encloses some  $\mathbf{B}$  field) will be infinite. It follows that (because the contour of integration is arbitrary) the current density  $\mathbf{J}_f$  will be infinite. Because this is not physically reasonable, we argue that the flux density  $\mathbf{B}$  remains zero just after the switch  $S$  is opened or that the condition of (7.1.16) holds. If the contour encloses the boundary at  $z = 0$  or  $z = d$ , the term on the right is infinite, thus indicating an infinite  $\mathbf{J}_f$ , which is actually a finite surface current density necessary to terminate the  $B_o$  field. This mathematical idealization results from the assumption that the external flux density  $B_o$  is established in zero time. In a real situation the flux density  $B_o$  will be established rapidly but at a finite rate. This idealization is better understood after the solution is completed. The process is analogous to the use of singularity functions in circuit theory to simplify mathematical analyses.

It should be clear that after a sufficiently long time all transient currents in the slab will die out and the flux density will be uniform throughout the slab,

$$\text{as } t \rightarrow \infty, \quad B_x = B_o, \quad (7.1.17)$$

for then  $\partial B_x / \partial t = 0$  in (7.1.15) for steady-state conditions.

To effect a solution of this problem we assume a separable solution of the form

$$B_x = \hat{B}(z)e^{-\alpha t} + B_0. \quad (7.1.18)$$

Substitution of this expression into 7.1.15 and cancellation of the exponential factor yields

$$\frac{1}{\mu_0\sigma} \frac{d^2\hat{B}}{dz^2} = -\alpha\hat{B}. \quad (7.1.19)$$

This equation has a solution

$$\hat{B} = C_1 \sin \sqrt{\mu_0\sigma\alpha} z + C_2 \cos \sqrt{\mu_0\sigma\alpha} z. \quad (7.1.20)$$

Thus the general solution is

$$B_x = (C_1 \sin \sqrt{\mu_0\sigma\alpha} z + C_2 \cos \sqrt{\mu_0\sigma\alpha} z)e^{-\alpha t} + B_0. \quad (7.1.21)$$

This equation must satisfy the initial conditions illustrated in the sketch of  $B_x$  as a function of  $z$  in Fig. 7.1.3. We can achieve this by setting

$$C_2 = 0$$

and expanding the rectangular distribution in a Fourier sine series.

Using the initial condition expressed by (7.1.16) and illustrated in Fig. 7.1.3, we write  $B_x(z, 0^+)$  as

$$0 = \sum_{n=1}^{\infty} a_n \sin \frac{n\pi z}{d} + B_0. \quad (7.1.22)$$

Comparison of (7.1.21) with  $C_2 = 0$  and (7.1.22) shows that each term in the series has

$$\alpha_n = \frac{n^2\pi^2}{\mu_0\sigma d^2} \quad (7.1.23)$$

We evaluate the coefficients  $a_n$  in the standard way by multiplying both sides

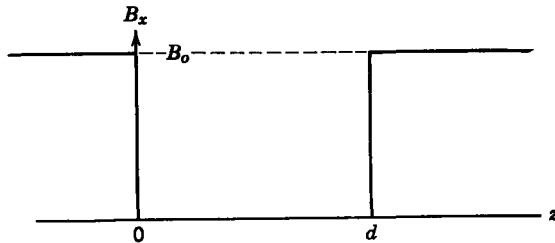


Fig. 7.1.3 Distribution of  $B_x$  at  $t = 0^+$  in the conducting slab of Fig. 7.1.2. The magnetic field distribution for  $t > 0$  is shown in Fig. 7.1.4.

(7.1.22) by  $\sin m\pi z/d$  and integrating

$$\int_0^d -B_o \sin \frac{m\pi z}{d} dz = \int_0^d \sum_{n=1}^{\infty} a_n \sin \frac{n\pi z}{d} \sin \frac{m\pi z}{d} dz. \quad (7.1.24)$$

All of the terms on the right for which  $m \neq n$  integrate to zero. Thus (7.1.24) reduces to

$$\int_0^d -B_o \sin \frac{n\pi z}{d} dz = \int_0^d a_n \sin^2 \frac{n\pi z}{d} dz. \quad (7.1.25)$$

Evaluation of the integral yields

$$\begin{aligned} a_n &= -\frac{4}{n\pi} B_o, & n \text{ odd,} \\ a_n &= 0, & n \text{ even,} \end{aligned} \quad (7.1.26)$$

and we write the complete solution for  $B_x$  as

$$B_x = B_o \left( 1 - \sum_{n \text{ odd}} \frac{4}{n\pi} \sin \frac{n\pi z}{d} e^{-\alpha_n t} \right). \quad (7.1.27)$$

In the solution (7.1.27) we see that each space harmonic damps at a different rate, the higher harmonics damping faster. We define the fundamental time constant  $\tau$  as

$$\tau = \frac{1}{\alpha_1} = \frac{\mu_0 \sigma d^2}{\pi^2} \quad (7.1.28)$$

and write (7.1.27) as

$$B_x = B_o \left( 1 - \sum_{n \text{ odd}} \frac{4}{n\pi} \sin \frac{n\pi z}{d} e^{-n^2 t/\tau} \right). \quad (7.1.29)$$

The fundamental time constant of (7.1.28), which is the longest time constant of the series, is usually called the *diffusion time constant* of the system.

The distribution of flux density, as expressed by (7.1.29), is plotted for several instants of time in Fig. 7.1.4. At  $t = 0$  the magnetic flux is excluded completely from the interior of the slab. As time progresses the flux diffuses into the slab. Because the higher space harmonics damp out faster, only three terms in the series are needed to calculate the curve at  $t = 0.1\tau$ ; only two terms are necessary for  $t = 0.3\tau$ ; and only the first term has appreciable value for  $t > \tau$ . Thus it is clear why the fundamental diffusion time  $\tau$  is the controlling time constant in the diffusion process. It is also clear from Fig. 7.1.4 that the field has almost completely diffused into the slab in a time  $t > 3\tau$ .

It is also instructive to investigate the behavior of the current density inside the slab during this transient diffusion process. The currents created by

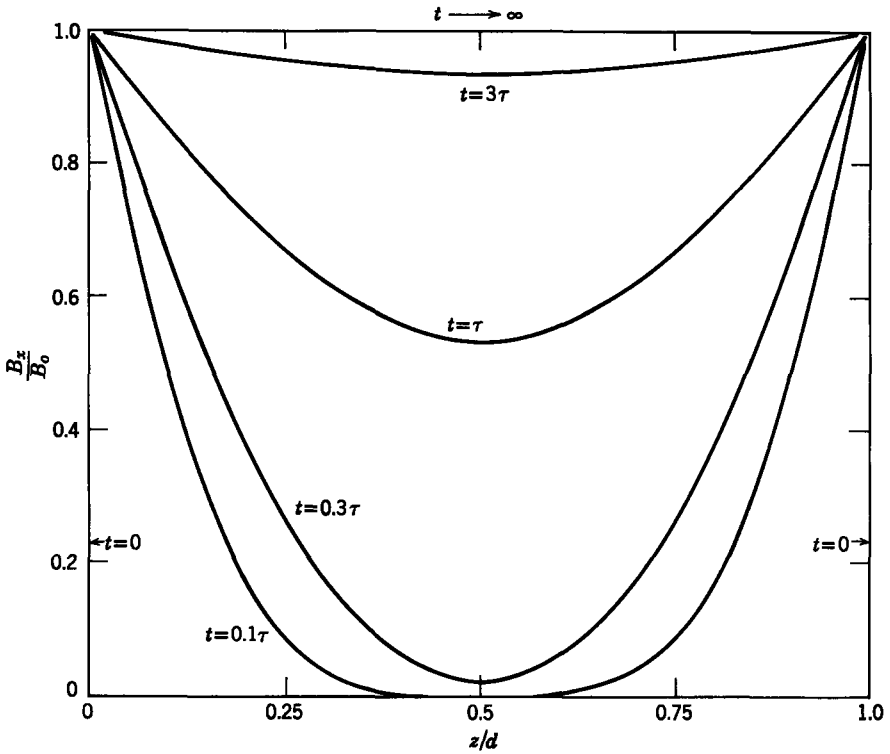


Fig. 7.1.4 Transient, one-dimensional diffusion of a magnetic field into a conducting material. The slab of conductor shown in Figs. 7.1.1 and 7.1.2 is viewed here from the end, as shown in Fig. 7.1.2.

induction in this way are often called *eddy currents*. We use (7.1.7) with the definitions of our present one-dimensional example (see Fig. 7.1.2) to obtain

$$J_y = \frac{1}{\mu_0} \frac{\partial B_x}{\partial z} = -\frac{B_0}{\mu_0 d} \sum_{n \text{ odd}} 4 \cos \frac{n\pi z}{d} e^{-n^2 t/\tau}. \quad (7.1.30)$$

The space distribution of this current density is plotted for several instants of time in Fig. 7.1.5. Note that at  $t = 0$  the series does not converge at  $z = 0$  and  $z = d$ . This shows that at  $t = 0$  the magnetic field is excluded completely from the slab and, to terminate the external tangential field, a surface current density is required [see (6.2.14)]\*. A surface current density implies an infinite volume current density; thus at  $t = 0$  there are impulses of  $J_y$  at  $z = 0$  and  $z = d$ , as shown in Fig. 7.1.5. As time progresses, the currents diffuse into the slab and decay. At the surface of the slab ( $z = 0$  or  $z = d$ ) the current density decays continuously, but at an interior point the current density increases from zero to some maximum value and decays back to zero.

\* Table 6.1, Appendix E.

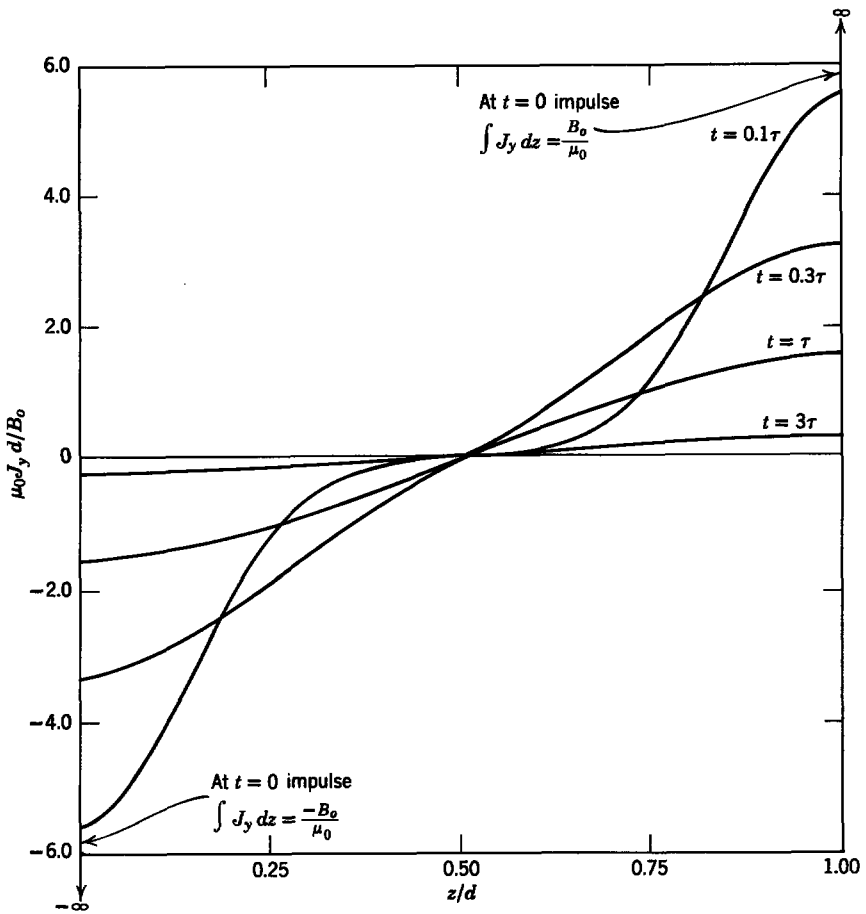


Fig. 7.1.5 Current distribution in transient one-dimensional diffusion.

Conservation of current requires that the current that flows down one side of the block must return on the opposite side. Hence the current distribution of Fig. 7.1.5 has odd symmetry about  $z = d/2$ . Note that the one-dimensional solution implies perfectly conducting end plates on the slab to provide a return path for the currents.

It should be clear from a study of Figs. 7.1.4 and 7.1.5 that if we are interested in electromagnetic phenomena that occur outside the slab and that have characteristic times much shorter than the diffusion time  $\tau$  we can approximate the properties of the slab by saying that  $\sigma \rightarrow \infty$ . In this approximation the flux is excluded from the interior of the slab and currents flow on the surfaces.

On the other hand, when we are concerned with phenomena with characteristic times that are long compared with the diffusion time  $\tau$ , we can

neglect perturbations due to diffusion effects for field calculations. These two limiting cases are illuminated more thoroughly in additional examples to follow. They are analogous to the constant current and constant flux conditions of the lumped-parameter system described in Section 5.1.3.

We can now state the physical conditions necessary for our mathematical idealization to be accurate. If the flux density  $B_0$  produced by current in the winding in Fig. 7.1.1 builds up in a time much smaller than the diffusion time constant, then our approximation of the boundary conditions at  $t = 0^+$  is valid. In any case, the mathematical model is least accurate for very small time, as should be evident from a careful comparison of the results of the analysis with physical reasoning about the sequence of events in a real system.

To illustrate the range of diffusion time constants that may be encountered with conducting media conventionally used in electromechanical systems (7.1.28) is used to obtain the plots of diffusion time constants as functions of slab thickness shown in Fig. 7.1.6. For a slab of copper 1 cm thick the diffusion time constant is approximately 1 msec, whereas for a seeded combustion gas, 1 m thick, the time constant is approximately 10  $\mu$ sec. Note that although the conductivity of silicon iron is more than an order of magnitude less than that of copper the diffusion time is longer because the permeability is so high. [In general  $\mu_0 \rightarrow \mu$  in (7.1.28) for magnetizable materials.] It is this long diffusion time that makes lamination of iron cores necessary in ac equipment of all types.

Because magnetic diffusion is described basically by Maxwell's equations, it occurs in both lumped-parameter and continuum systems. The analyses of Section 5.1.3 described magnetic diffusion in lumped-parameter systems, although this terminology was not used there. It is often helpful when considering continuum systems to reason qualitatively in terms of lumped-parameter models. Consequently, we consider a lumped-parameter system that provides an approximation of the diffusion process just discussed.

The conducting block of Fig. 7.1.1 is replaced with two perfectly conducting sheets short-circuited at one end and connected at the other end by a conductance  $G$ , as shown in Fig. 7.1.7. If, as before, we ignore fringing, the flux densities  $B_1$  and  $B_2$  are related to the currents by

$$B_2 = \frac{\mu_0 N i_2}{w}, \quad (7.1.31)$$

$$B_1 = \frac{\mu_0 N i_2}{w} - \frac{\mu_0 i_1}{w}, \quad (7.1.32)$$

where  $i_2$  is the coil current in Fig. 7.1.1. Then the flux linked by the terminals

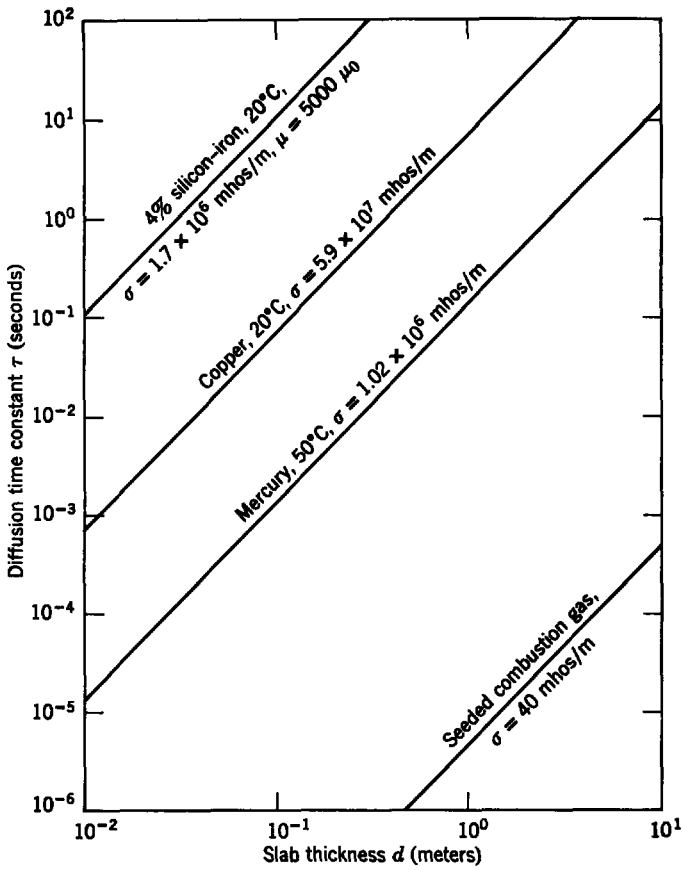


Fig. 7.1.6 Diffusion time constants  $\mu\sigma d^2/\pi^2$ .

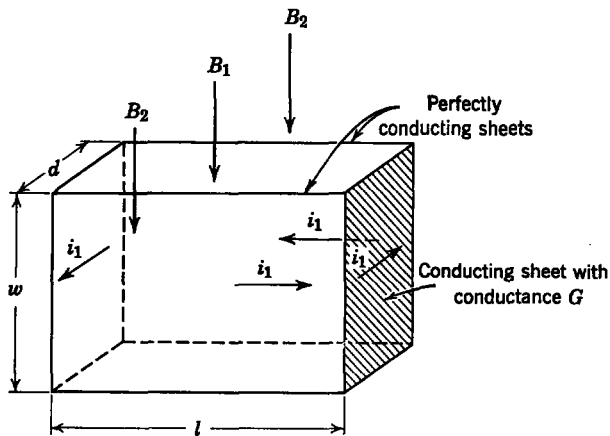


Fig. 7.1.7 A one-turn inductor used to replace the conducting block in Fig. 7.1.1.

of the inductor formed by the conducting sheets is

$$\lambda_1 = -dlB_1 = Li_1 - Mi_2, \tag{7.1.33}$$

where

$$L = \frac{dl\mu_0}{w},$$

$$M = \frac{dl\mu_0 N}{w}.$$

The circuit equation is then

$$GL \frac{di_1}{dt} + i_1 = GM \frac{di_2}{dt}. \tag{7.1.34}$$

In our example the current  $i_2$  is a step function of magnitude  $I$ . Hence the solution to (7.1.34) for  $i_1$  is

$$i_1 = INe^{-t/GL}, \tag{7.1.35}$$

where the definitions of  $L$  and  $M$  have been used.

The flux densities follow from (7.1.31) and (7.1.32). Outside the conductors for  $t > 0$ ,

$$B = B_2 = \frac{\mu_0 NI}{w}, \tag{7.1.36}$$

whereas between the conductors

$$B = B_1 = \frac{\mu_0 NI}{w} (1 - e^{-t/GL}). \tag{7.1.37}$$

This distribution of flux is shown in Fig. 7.1.8. When the switch is closed, there is no magnetic field between the conductors and a current exists to exclude the field. Then the interior region fills up with magnetic field at a

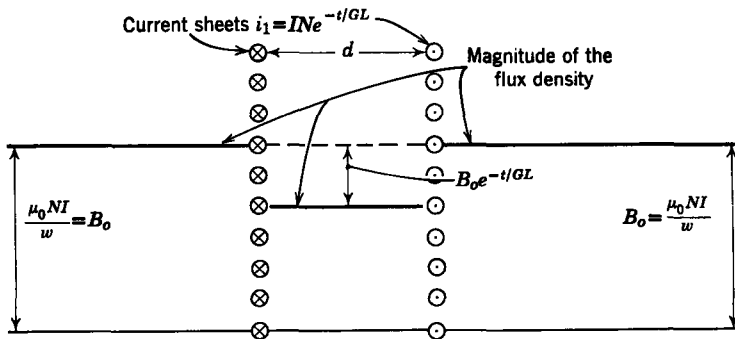


Fig. 7.1.8 Distribution of flux density as predicted by a lumped-parameter model.

rate characterized by the time constant  $GL$ . These distributions of current and flux density should be compared with those shown in Figs. 7.1.4 and 7.1.5.

If the equivalent  $G$  were computed as the dc conductance of the two sheets with length  $l$  and width  $w$  by using as the thickness  $2d/\pi^2 = 0.203d$ , we have

$$G = \left[ \frac{\sigma(2d/\pi^2)w}{2l} \right],$$

and using the value of  $L$  (7.1.33) the time constant is

$$GL = \frac{\mu_0 \sigma d^2}{\pi^2}.$$

or that predicted by the diffusion equation as the fundamental time constant of the system (7.1.28). Obviously, we would not know what thickness to use unless we had solved the exact problem, hence our lumped-parameter model can at best serve to interpret the diffusion process in terms of familiar lumped-parameter concepts. For engineering purposes, however, judiciously chosen lumped parameters provide a convenient and powerful model for many situations.

## 7.1.2 Diffusion and Steady Motion

As pointed out in the introduction, if the magnetic Reynolds number (7.0.4) is significant compared with unity, material motion can be responsible for altering current paths, hence redistributing the magnetic field. This type of phenomenon is best emphasized by considering situations in which the fields and motion are in a steady-state condition. Then the appropriate expression for the flux density is (7.1.12) with the velocity  $\mathbf{v}$  independent of time.

### 7.1.2a Steady-State in the Fixed Frame

The system depicted schematically in Fig. 7.1.9 is an example of the kind of steady-state diffusion problem we must consider when studying magneto-hydrodynamic (MHD) generators (see Chapter 12). It involves a continuous strip of material with constant  $\sigma$ ,  $\epsilon_0$ ,  $\mu_0$  which slides with constant velocity between a parallel pair of highly conducting electrodes. The sliding strip makes perfect electrical contact with the electrodes. The dimensions and coordinate system used are shown in Fig. 7.1.9. The system is excited at the end  $z = l$  by two current sources that supply a total current  $I$  to the electrodes. We wish to find the distribution of magnetic flux density in the sliding strip and study how it varies with system parameters.

To simplify the problem we assume that  $l/d$  and  $w/d$  are large enough

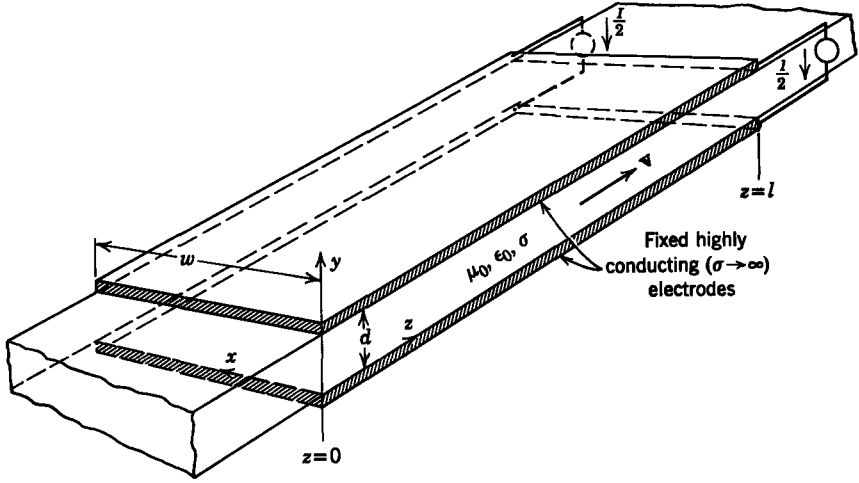


Fig. 7.1.9 Geometry for studying diffusion in the presence of steady motion.

that end and edge effects can be neglected.\* Thus the flux density will have only an  $x$ -component

$$\mathbf{B} = \mathbf{i}_x B_x, \tag{7.1.38}$$

the electric field intensity and current density will have only  $y$ -components

$$\mathbf{J} = \mathbf{i}_y J_y, \tag{7.1.39}$$

$$\mathbf{E} = \mathbf{i}_y E_y, \tag{7.1.40}$$

and the variables will not be functions of  $x$  or  $y$ ,

$$\frac{\partial}{\partial x} = \frac{\partial}{\partial y} = 0.$$

We have already specified that the strip is moving with constant velocity in the  $z$ -direction

$$\mathbf{v} = \mathbf{i}_z v_z. \tag{7.1.41}$$

Finally, interest is confined to a steady-state problem ( $\partial/\partial t = 0$ ).

With the given specifications, the  $x$ -component of (7.1.12) is

$$\frac{d^2 B_x}{dz^2} - \mu_0 \sigma v_z \frac{dB_x}{dz} = 0. \tag{7.1.42}$$

We have written total derivatives because  $B_x$  is a function only of  $z$ .

\* Standard practice in the analysis of MHD machines is to assume no fringing, solve the problem, and then add end effects as a perturbation. The end effect analysis is done by using conformal mapping techniques. See, for example, G. W. Sutton and A. Sherman, *Engineering Magnetohydrodynamics*, McGraw-Hill, New York, 1965, pp. 504–508.

Using the excitation of Fig. 7.1.9 and the boundary conditions of Table 6.1\*, we arrive at the conditions on the flux density

$$\text{at } z = 0, \quad B_x = 0, \quad (7.1.43a)$$

$$\text{at } z = l, \quad B_x = \frac{\mu_0 I}{w}. \quad (7.1.43b)$$

First consider the system with the velocity equal to zero. The solution for the flux distribution is

$$B_x = \frac{\mu_0 I}{w} \frac{z}{l}. \quad (7.1.44)$$

The distribution of current density is found from the  $y$ -component of (7.1.7),

$$J_y = \frac{1}{\mu_0} \frac{dB_x}{dz}, \quad (7.1.45)$$

and for zero velocity it is

$$J_y = \frac{I}{wl}. \quad (7.1.46)$$

This uniform current density and linearly varying flux density are what we expect in the absence of motion

When the velocity is finite, solutions for (7.1.42) are of the form

$$B_x = C e^{rz}$$

Substitution into (7.1.42) and cancellation of common factors gives

$$r^2 - \mu_0 \sigma v_z r = 0.$$

The solutions for this equation are

$$r = \mu_0 \sigma v_z, 0,$$

which yield the general solution for  $B_x$

$$B_x = C_1 + C_2 e^{R_m(z/l)}, \quad (7.1.47)$$

where we have again defined the *magnetic Reynolds number*  $R_m$  as

$$R_m = \mu_0 \sigma v_z l. \quad (7.1.48)$$

The significance of this number in the present context is discussed later.

Using the boundary conditions of (7.1.43), the constants  $C_1$  and  $C_2$  in (7.1.47) are evaluated to obtain the solution

$$B_x = \frac{\mu_0 I}{w} \left[ \frac{e^{R_m(z/l)} - 1}{e^{R_m} - 1} \right]. \quad (7.1.49)$$

\* See Appendix E.

The distribution of current density is evaluated by using this result in (7.1.45):

$$J_y = \frac{I}{wl} \left[ \frac{R_m e^{R_m(z/l)}}{e^{R_m} - 1} \right]. \tag{7.1.50}$$

Note that as  $R_m \rightarrow 0$  these expressions reduce to those of (7.1.44) and (7.1.46), which were derived by assuming zero velocity.

The flux density and current density are plotted as functions of position for several values of magnetic Reynolds number  $R_m$  in Fig. 7.1.10. It is evident from these curves that the higher  $R_m$ , the more flux density and current density are distorted, both being decreased at the entrance to the electrodes. It was shown in Section 7.1.1 that when we try to change the flux density in a conductor eddy currents flow to oppose the flux change. The eddy currents decay and the flux diffuses into the conductor in the process characterized by a diffusion time constant.

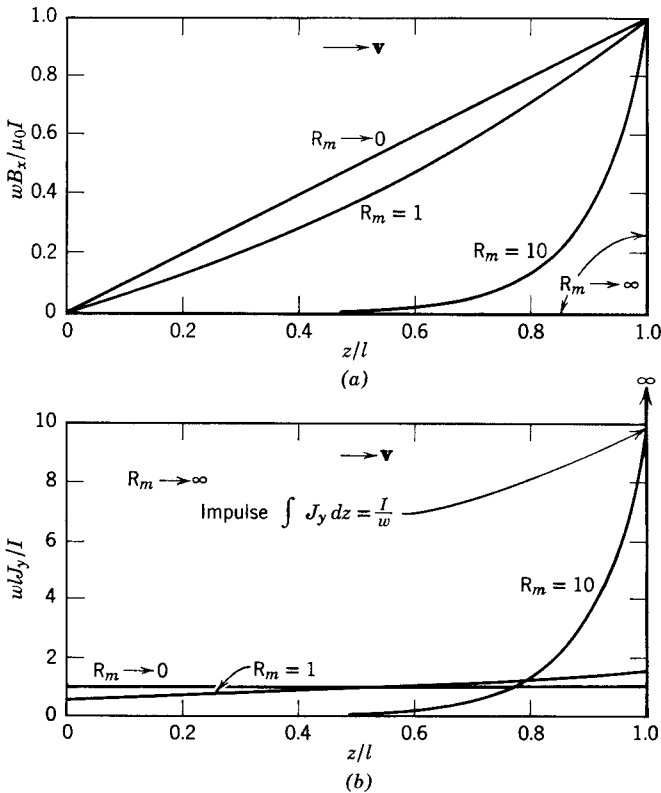


Fig. 7.1.10 Distribution of flux density and current density in the system of Fig. 7.1.9: (a) flux density; (b) current density.

If, in the system of Fig. 7.1.9, we view what happens to a particular sample of the moving strip, we see the competing processes of the sample trying to sweep the flux and current in the direction of motion and the diffusion of flux and current in the opposite direction. The magnitude of the magnetic Reynolds number is an indicator of the relative effectiveness of the two processes; a large  $R_m$  indicates a relatively slow diffusion process. We can interpret the magnetic Reynolds number as being proportional to the ratio of the diffusion time constant to the time it takes a sample of material to traverse the length of the electrodes. Equation 7.1.28 is used to write the diffusion time constant for the length  $l$  as

$$\tau_d = \frac{\mu_0 \sigma l^2}{\pi^2}.$$

The time taken for a sample of material to traverse the length  $l$  with speed  $v_z$  is

$$\tau_t = \frac{l}{v_z}.$$

The ratio of diffusion time constant to traversal time is then

$$\frac{\tau_d}{\tau_t} = \frac{\mu_0 \sigma v_z l}{\pi^2} = \frac{R_m}{\pi^2}.$$

The magnetic Reynolds number was defined in a particular way for this example. We find in our further studies of quasi-static magnetic field systems that it is useful to define magnetic Reynolds numbers in other ways; the fundamental interpretation, however, is always the same, namely that a magnetic Reynolds number indicates the relative importance of the diffusion ( $\nabla^2 \mathbf{B}$ ) and convection  $\nabla \times (\mathbf{v} \times \mathbf{B})$  terms in (7.1.12).

### 7.1.2b Steady State in the Moving Frame

The steady-state diffusion situation considered in the preceding subsection could be viewed from a frame moving with the conductor, in which case the magnetic field would be in a transient condition but the velocity  $v_z$  would be zero. Here, we turn this relationship around and consider a problem that is in a transient state in the fixed frame but in the steady state in the moving frame. The example provides further insight into the significance of the magnetic Reynolds number.

In the introduction to this chapter (see Fig. 7.0.1c) we discussed an example in which a block of conducting material moves with the velocity  $V$  between short-circuited, perfectly conducting parallel plates. If the current excitation in that problem is used to establish the field and is then instantaneously removed, currents will continue to flow through the block and the shorting

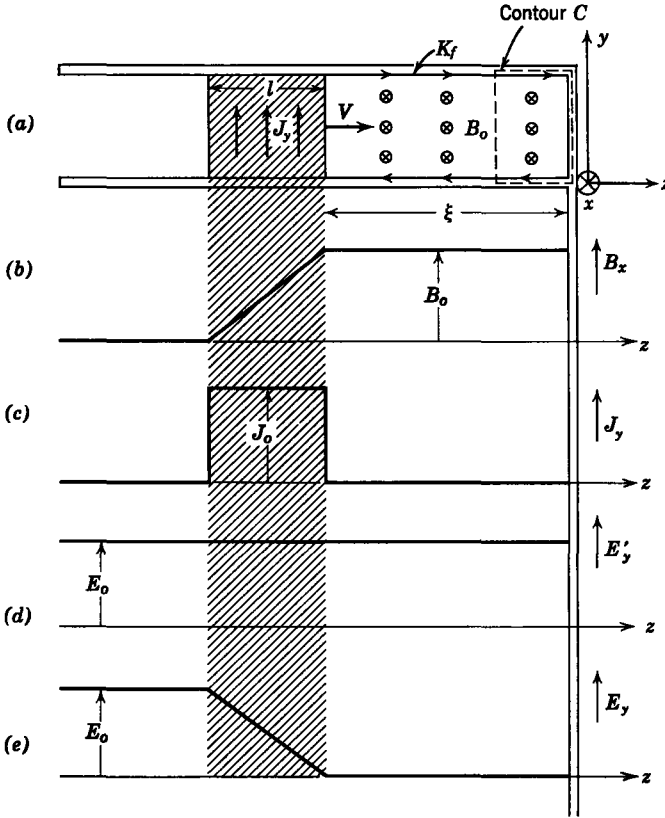


Fig. 7.1.11 The conducting block moves with just the velocity  $V$  required to maintain the flux density  $B_0$  constant. This velocity is such that  $R_m = 1$ .

end plate, as shown in Fig. 7.1.11a. Then there is a magnetic field ahead of the moving block of conductor but none behind.

Now, if the block were stationary, the magnetic field within the “inductor” formed by the block and the perfectly conducting plates would decay, much as in the example in Section 7.1.1. It is possible, however, for the block to move to the right with a sufficient velocity  $V$  to maintain the flux density  $B_0$  ahead of the block constant. Under this circumstance the fields can be found by observing that in the frame of the block the situation is no different than for a static case in which the field to the right is constant and the field to the left is zero; that is, in the frame of the moving block,

$$\mathbf{J}' = J'_y \mathbf{i}_y = \text{constant} = \sigma E'_y \mathbf{i}_y \tag{7.1.51}$$

for  $-(\xi + l) < z < -\xi$ .

Remember that the flux density generated by this current is the same in either the fixed or moving frame (see Table 6.1)\*. Hence

$$\mathbf{B}' = \mathbf{B} = \mathbf{i}_x B_o \frac{(z + \xi + l)}{l} \quad (7.1.52)$$

for  $-(\xi + l) < z < -\xi$  and

$$\mathbf{B} = B_o \mathbf{i}_x \quad (7.1.53)$$

for  $-\xi < z < 0$ . The flux density and current density are sketched in Fig. 7.1.11*b, c*. Here the gap length  $\xi = -Vt + \text{constant}$ , where  $V$  is a constant.

There is no time rate of change of the flux enclosed by a fixed contour (such as  $C$  in Fig. 7.1.11*a*) that passes through the perfectly conducting plates and the region ahead of the moving block. Hence

$$\oint_C \mathbf{E} \cdot d\mathbf{l} = 0 \quad (7.1.54)$$

around this contour and  $E_y$  ahead of the block is zero. It follows from the transformation for the electric field (see Table 6.1)\* that

$$E'_y(z = -\xi) = (\mathbf{v} \times \mathbf{B})_y = VB_o. \quad (7.1.55)$$

A sketch of the distribution of  $E'_y$  is shown in Fig. 7.1.11*d*.

Of course, the surface current density  $K_f$  (which is equal to  $K'_f$  in a magnetic field system) is related to the flux density  $B_o$  (Ampère's law)

$$B_o = \mu_o K_f \quad (7.1.56)$$

and the surface current density in the perfectly conducting plates is also related to the current density in the block

$$K_f = J_y l. \quad (7.1.57)$$

If we now combine (7.1.51) with these last three equations, we obtain

$$\sigma V B_o = \frac{B_o}{\mu_o l}, \quad (7.1.58)$$

from which it follows that to obtain a constant magnetic flux density ahead of the moving block we must have

$$\mu_o \sigma V l = R_m = 1. \quad (7.1.59)$$

The distribution of electric field in the moving and fixed frames is shown in Fig. 7.1.11*d, e*. Note that in the region to the left  $E'_y = E_y$ , because there is no magnetic field in that region.

Now that the fields have been found, it is possible to write them in the fixed frame [in which they are functions of  $(z, t)$ ] and see that they satisfy (7.1.9).

Of course, what we have found is the solution for a particular value of  $V$ . The postulated steady-state condition in the moving frame prevails only if

\* See Appendix E.

(7.1.59) is satisfied. We know that the field decays to zero if the block is stationary, hence we conclude that if the velocity  $V$  is less than required to make  $R_m = 1$  the field ahead of the block will decay. More interesting is the fact that if  $V$  exceeds the value required to make  $R_m = 1$  the magnetic field ahead of the block will increase. In this case the block literally acts as a magnetic piston that compresses the magnetic field in the region bounded by the perfectly conducting plates and increases the flux density. This provides a mechanism for mechanical amplification of flux density which has been used with chemical explosives to achieve amplification by more than a factor of 10 (from 2 Wb/m<sup>2</sup> to 30 Wb/m<sup>2</sup>).\*

To establish a numerical idea when the conditions of (7.1.59) are met, it is helpful to recognize that this condition can also be written as

$$\frac{l}{V} = \pi^2 \tau,$$

where  $\tau$  is the diffusion time, defined by (7.1.28), and plotted in Fig. 7.1.6 for several conductors as a function of the material thickness. The quantity  $l/V$  is the time required for the material to traverse a distance equal to its thickness. Hence, if we have a copper block with the thickness of 10 cm, it follows from Fig. 7.1.6 that a velocity of

$$V = \frac{l}{\pi^2 \tau} = 0.13 \text{ m/sec}$$

is required just to maintain the flux ahead of the block constant.

The use of a solid block in motion to concentrate magnetic flux mechanically implies a transient situation. For steady-state flux concentration a system has been proposed and tested in which the steady flow of a liquid metal conductor with  $R_m > 1$  concentrates the flux.†

Other instances of flux concentration by mechanical motion occur in plasma devices used in research on controlled thermonuclear reactions. In these devices energy from a capacitor bank drives and heats a plasma and the mechanical motion of the plasma compresses the magnetic field and increases the flux density.‡

In a very different physical situation superconducting solids have essentially infinite electrical conductivity; hence at even low velocities the magnetic

\* C. M. Fowler et al., "Flux Concentration by Implosion," *High Magnetic Fields*, H. Kolm et al., eds. M.I.T. Press, Cambridge, Mass., and Wiley, New York, 1962, pp. 269–276.

† H. H. Kolm and O. K. Mawardi, "Hydromagnet: A Self-Generating Liquid Conductor Electromagnet," *J. Appl. Phys.*, **32**, No. 7, 1296–1304 (July 1961).

‡ D. J. Rose and Melville Clark, Jr., *Plasmas and Controlled Fusion*, M.I.T. Press and Wiley, New York, 1961, p. 360.

Reynolds number  $R_m$  is essentially infinite. As a result, superconducting solids are used for mechanical amplification of flux density.\*

7.1.3 The Sinusoidal Steady State in the Presence of Motion

Some of the most significant practical applications of magnetic diffusion phenomena are made possible by introducing two characteristic dynamical times into a single system; for example, in Fig. 7.1.12 a thin sheet of conducting metal (conductivity  $\sigma$ ) moves to the right with the constant velocity  $V$ .

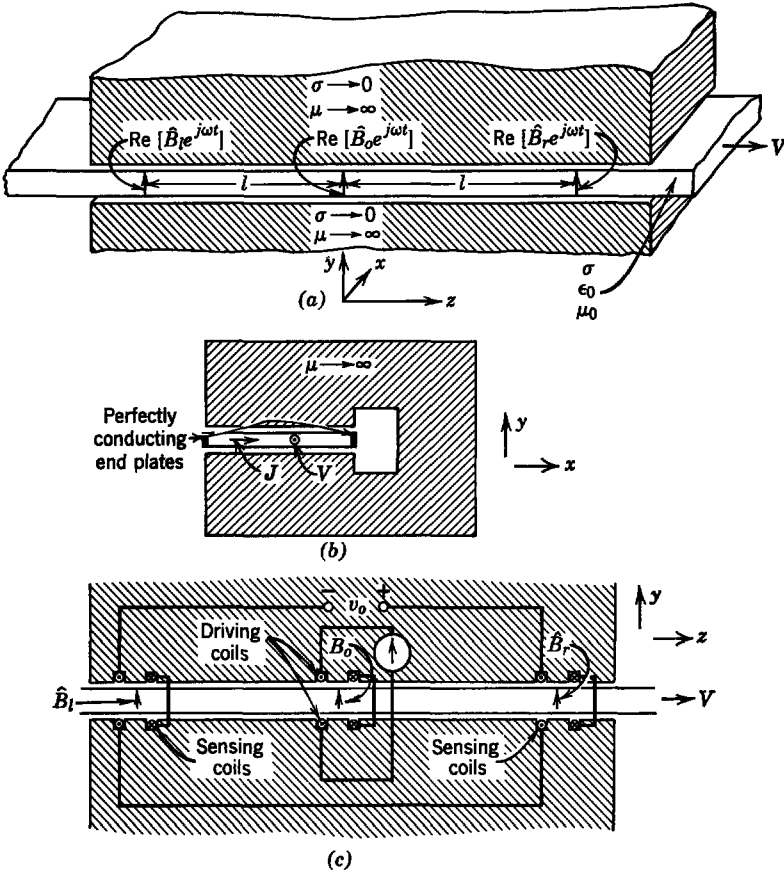


Fig. 7.1.12 (a) A thin slab of conductor moves to the right with velocity  $V$  in the air gap of a magnetic circuit; (b) end view of magnetic circuit showing a slab with perfectly conducting end plates moving out of paper; (c) excitation and detection circuits used to measure velocity  $V$  of the slab.

\* P. S. Swartz and C. H. Rosner, "Characteristics and a New Application of High-Field Superconductors," *J. Appl. Phys.*, 33, No. 7, 2292-2300 (July 1962).

External coils are used to impose the magnetic flux density

$$\mathbf{B} = \mathbf{i}_y \operatorname{Re} \left( \hat{B}_0 e^{j\omega t} \right) \quad (7.1.60)$$

at  $z = 0$ , as shown in Fig. 7.1.12*a*, *b*, *c*. In addition, coils are arranged symmetrically upstream and downstream from the excitation of (7.1.60). These coils are connected to a high impedance voltmeter, which measures the rms value of  $v_o$ , as shown in Fig. 7.1.12*c*. The coils are connected in series and in such a way that the voltage  $v_o$  is proportional to the difference between the time rates of change of  $B_r$  and  $B_l$ . With no motion, the device is symmetrical, and we expect that the output voltage  $v_o$  is zero. With motion we expect from the results of the preceding section that the conductor will tend to increase the flux density  $B_r$  and decrease  $B_l$ . If this is the case, the voltage  $v_o$  is a measure of the material velocity. Hence the system shown in Fig. 7.1.12 has the possibility of being a device to measure the velocity of the moving conducting sheet without making mechanical or electrical contact with the sheet.

The problem is particularly appropriate to our present discussion because it can be modeled by a one-dimensional diffusion problem. The sheet is assumed to move in the air gap of an infinitely permeable magnetic circuit so that fields  $B_y$  are returned through the circuit. Then currents are in the  $x$ -direction through the sheet and for our present purposes we can think of the sheet as having perfectly conducting end plates (Fig. 7.1.12*b*) which allow the currents to return through the sheet at other positions along the  $z$ -axis.

There are two characteristic times for the dynamics of this situation. First the excitation has the period  $2\pi/\omega$ , and we know from Section 7.1.1 that the relative value of this time and the diffusion time will be important. In addition, the motion introduces the characteristic time  $l/V$ , and from the studies undertaken in Section 7.1.2 we expect that this time in relation to the diffusion time will also be important.

We are interested in sinusoidal steady-state conditions, hence we require an expression for  $\mathbf{B}$  that includes both the effects of time varying fields and material motion. The appropriate equation is the  $y$ -component of (7.1.9), written with the assumption that  $\partial/\partial x = \partial/\partial y = 0$ . (Effects of the slots in which coils are placed are neglected.)

$$\frac{1}{\mu\sigma} \frac{\partial^2 B_y}{\partial z^2} = \frac{\partial B_y}{\partial t} + V \frac{\partial B_y}{\partial z}. \quad (7.1.61)$$

Note that these same assumptions require that a current be in the  $x$ -direction which from (7.1.7) is related to  $B_y$  by

$$J_x = -\frac{1}{\mu} \frac{\partial B_y}{\partial z}. \quad (7.1.62)$$

It is worthwhile to compare (7.1.61) to the one-dimensional diffusion equation for stationary media (7.1.15). The effect of the motion is to replace the time derivative with the convective derivative. Because  $B_y$  is the same, whether measured in the moving or the fixed frame, this result is reasonable. As we learned in Section 6.1, the terms on the right in 7.1.61 constitute the time rate of change of  $B_y$  for an observer moving with the material at the velocity  $V$ . Hence in the frame of the material (7.1.61) has the same physical significance as (7.1.15). In the present example, of course, the excitation is in the fixed frame and we cannot ignore the effect of the motion by solving the problem in the moving frame.

Because of the sinusoidal steady-state excitation (7.1.60), solutions to (7.1.61) are assumed to have the form

$$B_y = \text{Re} [\hat{B}(z)e^{j\omega t}]. \quad (7.1.63)$$

Substitution into (7.1.61) shows that this assumption is justified if

$$\frac{d^2 \hat{B}}{dz^2} - \mu\sigma V \frac{d\hat{B}}{dz} - j\omega\mu\sigma \hat{B} = 0. \quad (7.1.64)$$

This ordinary constant-coefficient equation can be solved by assuming solutions of the form  $\hat{B}(z) = e^{-jkz}$ . Then

$$k^2 - jk\mu\sigma V + j\omega\mu\sigma = 0. \quad (7.1.65)$$

Note that we could have obtained this expression, which is called the *dispersion equation*, by assuming both the temporal and spacial dependence at the outset and letting

$$B_y(z, t) = \text{Re} [\hat{B}_y e^{j(\omega t - kz)}]. \quad (7.1.66)$$

Solutions of this form satisfy (7.1.61), provided that  $\omega$  and  $k$  are related by (7.1.65). In the chapters that follow we make extensive use of solutions with this form. In the present situation  $\omega$  is a given real number. Then it is clear from (7.1.65) that the *wavenumber*  $k$  is complex. In solving (7.1.65), it is convenient to normalize  $k$  to the length  $l$ . There are then two possible wavenumbers ( $k = k^-$  and  $k = k^+$ ) for a given frequency  $\omega$ .

$$l(k^\mp) = \frac{jR_m}{2} \pm j \left[ \left( \frac{R_m}{2} \right)^2 + 2j \left( \frac{l}{\delta} \right)^2 \right]^{1/2} \quad (7.1.67)$$

Here the magnetic Reynolds number

$$R_m = \mu\sigma V l \quad (7.1.68)$$

and the *skin depth*  $\delta$ , defined by

$$\delta = \left( \frac{2}{\omega\mu\sigma} \right)^{1/2}, \quad (7.1.69)$$

have been introduced. By these definitions  $R_m$  represents the effect of the material velocity  $V$ , whereas  $\delta$  brings in the excitation frequency  $\omega$ . As can be seen from (7.1.67), the diffusion with no motion ( $R_m = 0$ ) is described by  $\delta$ , and it is worthwhile to consider this limiting case so that the effect of the motion can be fully appreciated.

### 7.1.3a Sinusoidal Steady State with No Motion (Skin Effect)

The sinusoidal steady-state diffusion of a magnetic field into a conductor assumes considerable importance outside the area of electromechanics; for example, the ac resistance of a stationary wire is significantly dependent on frequency,\* as are the losses in the walls of a waveguide.† In each of these cases the phenomenon is conventionally referred to as *skin effect* because the currents in the conductor tend to crowd into a region near the surface.

Skin-effect is a magnetic diffusion phenomenon. Section 7.1.1 was concerned with transient skin effect. It is exemplified here as the limiting case in which  $V = 0$  ( $R_m = 0$ ). Then from (7.1.67) the wavenumbers are (remember that  $\sqrt{j} = (1 + j)/\sqrt{2}$ )

$$k^{\mp} = \mp \frac{1 - j}{\delta}. \quad (7.1.70)$$

Now, if we substitute these wavenumbers into (7.1.66), we find that one of the solutions increases exponentially with  $z$  as the other decreases. For the present purposes we assume that the extremities of the system in the  $z$ -direction are sufficiently remote that the fields there have decayed to zero. Then, in the region to the right in Fig. 7.1.12, the appropriate solution is (here the wavenumber  $k^+$  is used)

$$B_y = \text{Re} [B_0 e^{-z/\delta} e^{j(\omega t - z/\delta)}]. \quad (7.1.71)$$

From this expression it is clear that there are two parts to the solution, as shown in Fig. 7.1.13. To illustrate some of the properties of this *diffusion wave*, the two factors of (7.1.71) are plotted in Fig. 7.1.13. Here, the excitation constant  $B_0$  is assumed to be real. Then the factor  $\cos(\omega t - z/\delta)$  represents a wave of constant amplitude, traveling in the positive  $z$ -direction. We define a *phase velocity*  $v_p$  for this constant-amplitude wave by calculating the velocity of a point of constant phase. The phase of an arbitrary point on the wave (e.g., point  $A$  in Fig. 7.1.13) remains constant for an observer at the position  $z$  such that

$$\omega t - z/\delta = \text{constant}. \quad (7.1.72)$$

\* S. Ramo, J. R. Whinnery, and T. Van Duzer, *Fields and Waves in Communication Electronics*. Wiley, New York, 1965, p. 194.

† *Ibid.* p. 379.

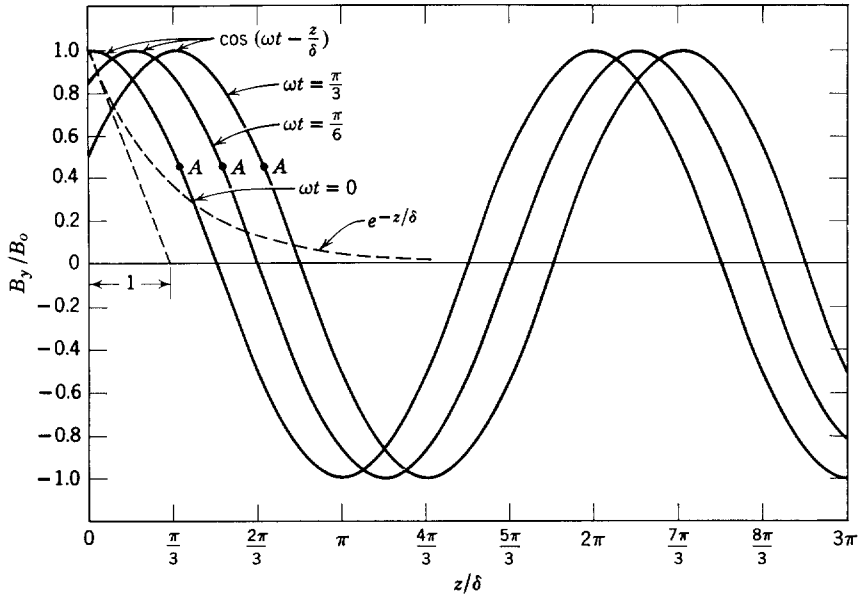


Fig. 7.1.13 Components of a diffusion wave.

To find the phase velocity we differentiate this expression with respect to time to obtain

$$v_p = \omega\delta. \quad (7.1.73)$$

Thus the point *A* or any other point of constant phase on the constant amplitude part of the wave will travel with a phase velocity  $\omega\delta$ .

The two factors plotted separately in Fig. 7.1.13 are multiplied and replotted to show the complete diffusion wave in Fig. 7.1.14. With the attenuation it is difficult to identify an arbitrary point of constant phase on the wave.

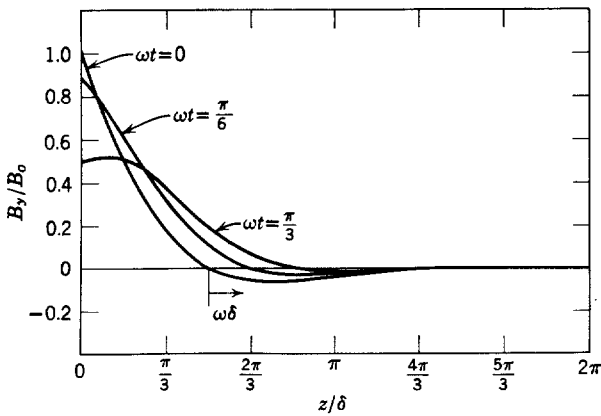


Fig. 7.1.14 A diffusion wave.

We can, however, always be unambiguous by defining the phase velocity in terms of the velocity of a zero-crossing.

A salient property of the diffusion wave is that the spacial rate of decay and the wavelength are both directly proportional to  $\delta$ ; that is, as can be seen from Fig. 7.1.13, the wave envelope has an extrapolated decay distance equal to the skin depth  $\delta$  and the wavelength  $\lambda = 2\pi\delta$ . Hence in Fig. 7.1.14 it is difficult to discern more than one point of zero amplitude.

It is important to recognize that a diffusion wave describes the dynamics of an essentially dissipative interaction. As we shall see in Chapter 10, sinusoidal steady-state waves can be excited in cases in which decay (or evanescence) occurs but there is no dissipation of energy.

In Section 10.1.4 we shall have occasion to return to diffusion waves in another context. There the “mushy” nature of these waves is emphasized.

Because the skin depth  $\delta$  is such a critical parameter in the electromagnetic

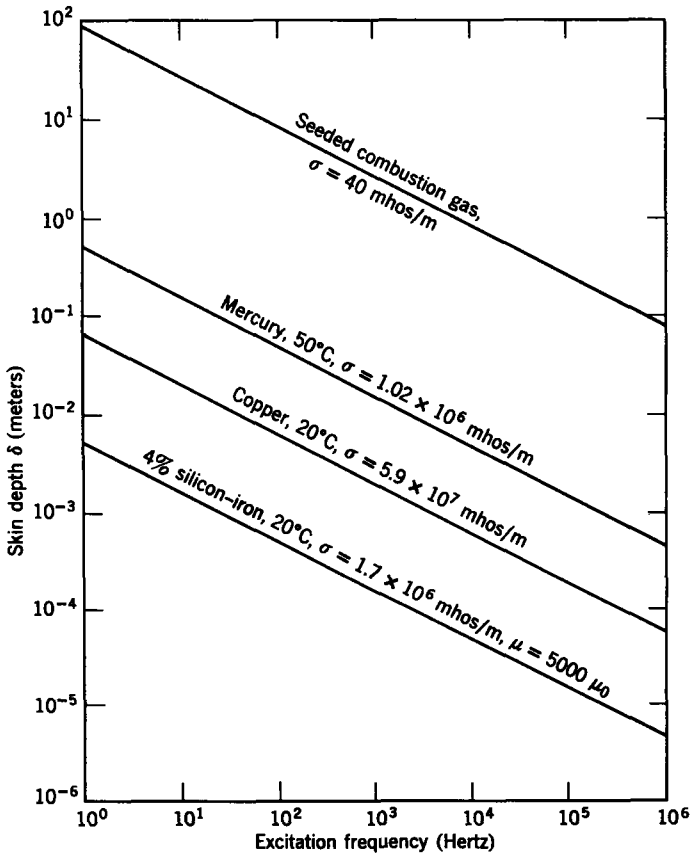
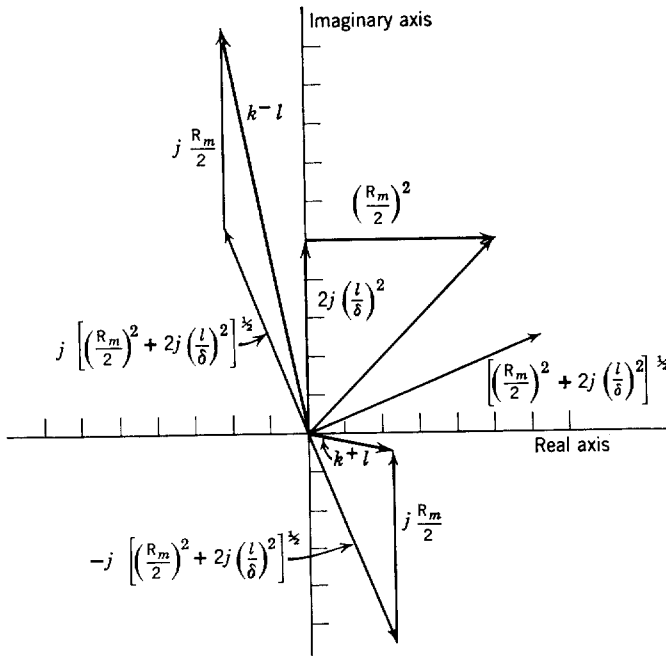


Fig. 7.1.15 Skin depth as a function of frequency for several typical materials.

behavior of conducting materials, it is worthwhile to calculate the skin depth for some typical materials. Equation 7.1.69 is used with the material constants in Fig. 7.1.6 to plot the curves of skin depths as functions of frequency shown in Fig. 7.1.15. Note the tremendous range of skin depths obtainable with useful materials; for example, in silicon iron, even at the low frequency of 1 Hz the skin depth is approximately  $\frac{1}{2}$  cm. It is quite clear from these plots that many situations exist in which it is appropriate to assume the material infinitely conducting ( $\delta \approx 0$ ). On the other hand, it is also clear that situations exist in which it is appropriate to neglect the skin effect and the induced currents. A comparison should be made between Figs. 7.1.15 and 7.1.6 because the skin depth and the diffusion time constant are closely related.

**7.1.3b The Effect of Motion**

To assess the effect of material motion on diffusion waves, the wavenumbers given by (7.1.67) must be considered for finite values of  $R_m$ . To determine the relative magnitudes of the real ( $k_r$ ) and imaginary ( $k_i$ ) parts of the wavenumber, it is helpful to construct the solution of (7.1.67) graphically (Fig. 7.1.16). From this construction it is clear that the real parts of



**Fig. 7.1.16** Graphical construction of solutions to (7.1.67) for the normalized complex wavenumbers  $k+l$  and  $k-l$ .

$k^+$  and  $k^-$  are negatives,

$$k_r^- = -k_r^+, \quad (7.1.74)$$

that  $k_i^-$  is positive and  $k_i^+$  is negative,

$$k_i^- > 0 > k_i^+, \quad (7.1.75)$$

and that the magnitude of  $k_i^-$  is greater than that of  $k_i^+$ ,

$$|k_i^-| > |k_i^+|. \quad (7.1.76)$$

The arguments in Section 7.1.3a concerning the extent of the system are then used to arrive at the solutions

$$B_y = \text{Re} [\hat{B}_o e^{-|k_i^+|z} e^{j(\omega t - |k_r^+|z)}] \quad (7.1.77)$$

for  $z > 0$  and

$$B_y = \text{Re} [\hat{B}_o e^{|k_i^-|z} e^{j(\omega t + |k_r^-|z)}] \quad (7.1.78)$$

for  $z < 0$ . From these solutions it is clear that to the right a diffusion wave still propagates in the  $+z$ -direction with a phase velocity  $\omega/|k_r^+|$  that is modified by the material motion. Moreover, in spite of the motion, a wave propagates to the left with this same phase velocity. The effect of the motion is most apparent in the rate of decay for these waves. The spacial rate of attenuation to the right is decreased by the motion, whereas that to the left is increased. An instantaneous view of the magnetic flux density amplitude to the right and left would appear as shown in Fig. 7.1.17.

As a practical application of the magnetic diffusion phenomenon we have considered in this section, the device shown in Fig. 7.1.12 is now used to measure the velocity of the material. The output voltage from the sensing coils has the form  $v_o = \text{Re} (\hat{v}_o e^{j\omega t})$ . The coils are connected so that in the absence of motion there is no output signal; that is,

$$\hat{v}_o = j\omega A [\hat{B}_y(l) - \hat{B}_y(-l)], \quad (7.1.79)$$

where  $A$  is a geometric constant that depends on the coil area and number of turns. The  $j\omega$  in (7.1.79) accounts for the voltage being the time rate of change of the flux. (Here we assume that not only do the coils support a negligible current so that they do not disturb the magnetic field but they have dimensions in the  $z$ -direction that are small compared with a wavelength  $2\pi/|k_r^-|$ .) In substituting the solutions given by (7.1.77) and (7.1.78) into (7.1.79), it is convenient to use first the complex wavenumbers  $k^+$  and  $k^-$ ,

$$\hat{v}_o = j\omega A \hat{B}_o (e^{-jk^+l} - e^{+jk^-l}) \quad (7.1.80)$$

because then we can use (7.1.67) to write this expression as

$$\hat{v}_o = j\omega 2A \hat{B}_o \sinh \left( \frac{R_m}{2} \right) \exp - \left[ \left( \frac{R_m}{2} \right)^2 + 2j \left( \frac{l}{\delta} \right)^2 \right]^{1/2}. \quad (7.1.81)$$

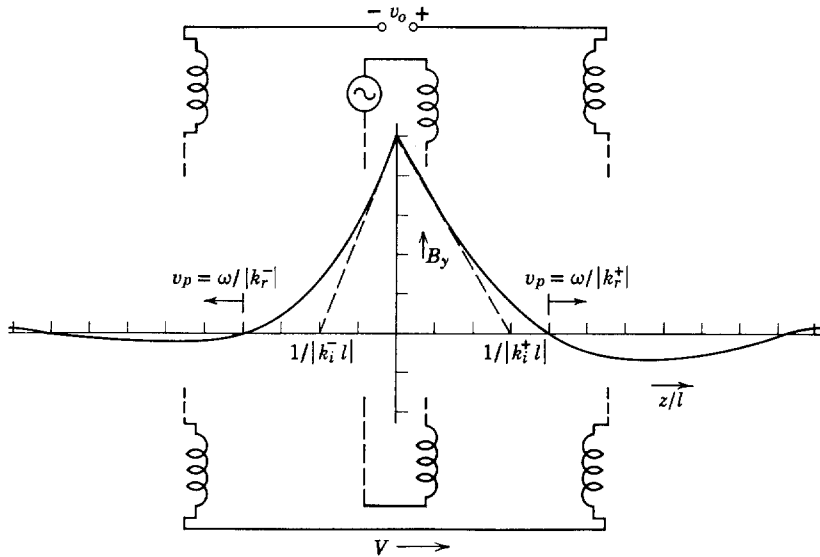


**Fig. 7.1.17** Instantaneous distribution of magnetic flux density in the moving slab of conductor shown in Fig. 7.1.12. Points of constant phase move to the right and left with equal velocities but attenuation to the right is decreased by motion, whereas that to the left is increased. Note that detailed account of the excitation at  $z = 0$  by the coil has not been made. Hence distribution of  $B_y$  at  $z = 0$  has a discontinuous slope.

From this equation it is apparent that as  $R_m$  approaches zero, the output voltage from the sensing coils does also. For small values of  $R_m/2$  compared with unity and  $l/\delta$  and for fixed frequency  $\omega$  the output voltage takes the form

$$\hat{v}_o = (\text{constant}) R_m; \quad (7.1.82)$$

that is, in this range of parameters, the voltage  $v_o$  is directly proportional to the velocity  $V$  of the moving conducting sheet.

The mechanism made available by this phenomenon for measuring the velocity of a material is attractive because it does not require mechanical or electrical contact with the moving medium. Also by varying the frequency the output voltage can be made to give information about the material conductivity.

Devices that exploit the interaction described here are used to measure rotational velocity with drag-cup tachometers\* and in flowmeters to measure

\* C. W. Blachford, "Induction Cup Parameters from Electromagnetic Field Theory and Experimental Analysis," *IEEE Trans. Power Apparatus Systems*, **PAS. 84**, No. 11, 189-193 (November 1965).

the velocity of liquid metals.\* Note that the output voltage is proportional to the conductivity of the moving medium ( $R_m = \mu_0 \sigma V l$ ). Hence there is a lower limit on the material conductivity that will lead to a useful output voltage.

**7.1.4 Traveling Wave Diffusion in Moving Media**

In Section 7.1.3 attention was given to the effect of material motion on the diffusion of magnetic fields excited in the sinusoidal steady state. These same ingredients are also present in the topic to be undertaken in this section, with attention now being given to currents and forces induced in the moving material. Figure 7.1.18 shows a slab of conducting material that can be moving to the right with velocity  $V$ . Adjacent to the lower surface, coils are distributed and interconnected in such a way that a surface current

$$\mathbf{K}_f = \text{Re} [K e^{j(\omega t - kz)} \mathbf{i}_x], \quad (K \text{ real}), \quad (7.1.83)$$

is excited. Hence at any point in the  $x$ - $z$  plane this current varies sinusoidally with the frequency  $\omega$ , whereas at any instant it varies sinusoidally in space. Points of constant phase on the current sheet move to the right with the velocity  $\omega/k$ , where both  $\omega$  and  $k$  are given.

This example has attributes that make it possible to demonstrate the basic mechanism responsible for several practical magnetic induction-type interactions. As we shall see, currents are induced in the conducting material.

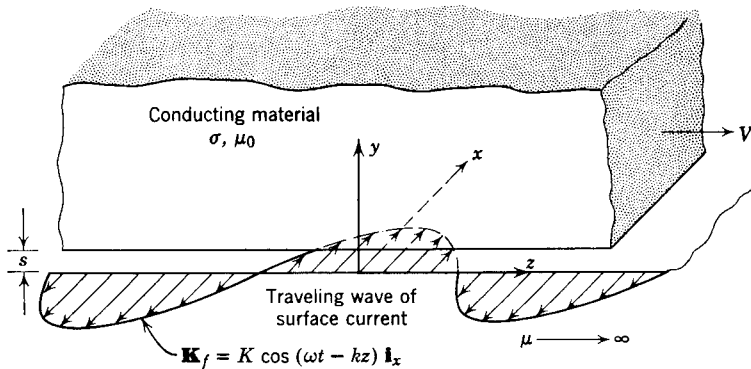


**Fig. 7.1.18** A slab of conducting material moves in the  $z$ -direction with velocity  $V$ . Just below the slab sinusoidally distributed windings are driven by a traveling wave of surface current density which has the phase velocity  $\omega/k$  to the right. It is assumed that an infinitely permeable material is just below the current sheet and that the extent of the conducting slab in the  $y$ -direction is many wavelengths  $2\pi/k$ .

\* For a discussion of magnetohydrodynamic flow measuring devices see J. A. Shercliff, *The Theory of Electromagnetic Flow Measurement*, Cambridge University Press (1962). In particular, the interaction described is basic to material beginning on p. 103.

These currents, and the associated magnetic fields, can produce a time average force on the material in the  $y$ -direction. This type of force is often used to levitate solid and liquid metals. Other forces are induced in the  $z$ -direction, and under certain conditions this makes it possible to pull the conducting material in the  $z$ -direction. This induced force is the basis for the induction machine discussed in Section 4.1.6b and is often used to pump liquid metals.

One of our main objectives in this section is to establish further insight into the manner in which currents and the magnetic fields distribute themselves in a moving conducting medium. The magnetic flux density is given by (7.1.9), which has the  $y$ -component

$$\frac{1}{\mu\sigma} \left( \frac{\partial^2 B_y}{\partial y^2} + \frac{\partial^2 B_y}{\partial z^2} \right) = \frac{\partial B_y}{\partial t} + V \frac{\partial B_y}{\partial z} \quad (7.1.84)$$

Hence we assume that the field distribution does not depend on the  $x$ -coordinate, and  $B_y$  is predicted by a diffusion equation with the same form as (7.1.61), except that now the magnetic field diffusion occurs in two dimensions. Once the component  $B_y$  has been found from (7.1.84), the remaining component  $B_z$  can be found from the relation  $\nabla \cdot \mathbf{B} = 0$ , which requires

$$\frac{\partial B_y}{\partial y} + \frac{\partial B_z}{\partial z} = 0. \quad (7.1.85)$$

The magnetic field is driven by the surface current of (7.1.83). Hence we look for solutions with the same traveling wave dependence on  $(z, t)$ ; that is, we assume that the flux density and the current density take the forms

$$\mathbf{B} = \text{Re} [(\hat{B}_y(y)\mathbf{i}_y + \hat{B}_z(y)\mathbf{i}_z)e^{j(\omega t - kz)}], \quad (7.1.86)$$

$$\mathbf{J} = \text{Re} [\hat{J}_x(y)\mathbf{i}_x e^{j(\omega t - kz)}].$$

It follows from (7.1.84) that in order for the solutions to take these forms  $\hat{B}_y$  must satisfy the equation

$$\frac{d^2 \hat{B}_y}{dy^2} - \alpha^2 \hat{B}_y = 0, \quad (7.1.87)$$

where

$$\alpha = k\sqrt{1 + jS},$$

$$S = \frac{\mu\sigma}{k^2} (\omega - kV).$$

The solutions to (7.1.87) are  $\exp \pm \alpha y$ . We have defined  $\alpha$  as having a positive real part. The  $y$ -dimension of the slab is assumed to be very large compared with a wavelength  $2\pi/k$ , and it is therefore appropriate to assume that the fields approach zero as  $y \rightarrow \infty$  with the dependence

$$\hat{B}_y = \hat{A}e^{-\alpha y}. \quad (7.1.88)$$

From (7.1.85) and the assumed form of solutions  $\hat{B}_z$  is given by

$$\hat{B}_z = \frac{1}{jk} \frac{d\hat{B}_y}{dy} = -\frac{\alpha\hat{A}}{jk} e^{-\alpha y}. \quad (7.1.89)$$

The constant  $\hat{A}$  is determined by the boundary condition imposed by the current sheet at  $y = 0$ . For purposes of simplicity it is assumed that the distance  $s$  between the current sheet and the lower surface of the conducting slab is small compared with the wavelength  $2\pi/k$  and that the current sheet is bounded from below by a highly permeable material. This means that

$$\hat{B}_z(0) = \mu_0 K. \quad (7.1.90)$$

These last two equations serve to define the constant  $\hat{A}$ , and it follows that the magnetic flux density in the moving conductor is

$$\mathbf{B} = \text{Re} \left[ \mu_0 K \left( \frac{-jk}{\alpha} \mathbf{i}_y + \mathbf{i}_z \right) e^{-\alpha y} e^{j(\omega t - kz)} \right]. \quad (7.1.91)$$

The current density implied by this flux density can be found from the relation  $\mathbf{J} = \nabla \times \mathbf{H}$ . In the present two-dimensional situation the only component of  $\mathbf{J}$  is

$$J_x = \frac{1}{\mu_0} (jk\hat{B}_y - \alpha\hat{B}_z), \quad (7.1.92)$$

and it follows from (7.1.91) that this is

$$J_x = \text{Re} \left[ \frac{-jKk^2 S}{\alpha} e^{-\alpha y} e^{j(\omega t - kz)} \right] \quad (7.1.93)$$

The component  $B_z$  of the flux density and the current density  $J_x$  are distributed in the conducting slab, as shown in Fig. 7.1.19. It is clear that the flux and current distributions are strongly dependent on the parameter  $S$ . To understand the significance of this parameter recall from Section 7.1.1 that the magnetic diffusion time based on the wavelength  $\lambda = 2\pi/k$  is (within a factor of 4)

$$\frac{\mu\sigma}{k^2},$$

whereas the rate of change with respect to time of  $B_y$  (say) for an observer moving with the velocity  $V$  of the slab is

$$\left( \frac{\partial}{\partial t} + V \frac{\partial}{\partial z} \right) B_y \rightarrow j(\omega - kV) \hat{B}_y;$$

that is,  $\omega - kV$  is the frequency of the magnetic flux density for an observer moving with the conducting slab. Hence  $S$  is (proportional to) the ratio of the magnetic diffusion time to the period of excitation in the frame of the moving medium.

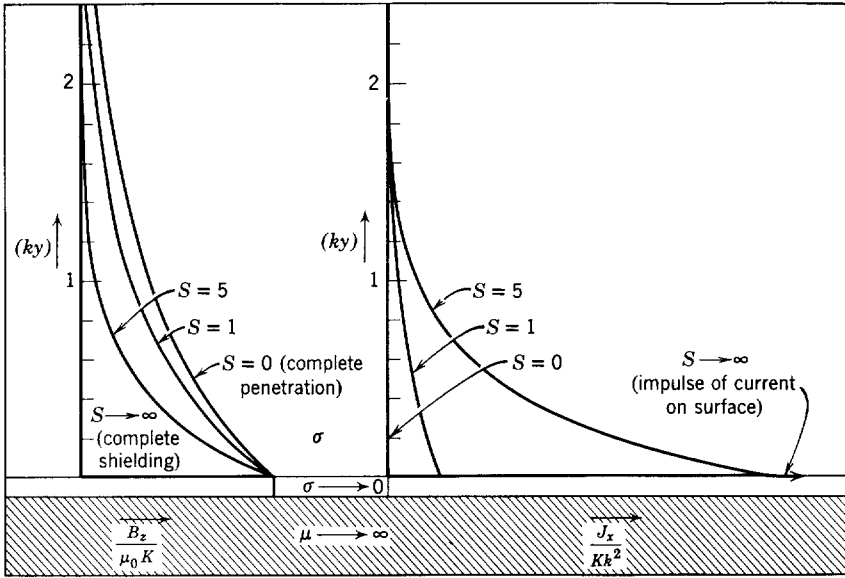


**Fig. 7.1.19** Distribution of the instantaneous magnitudes of  $B_z$  and  $J_x$  in the moving conducting slab of Fig. 7.1.18;  $S$  is defined following (7.1.87).

Because the phase velocity of the traveling wave is  $\omega/k$ ,  $S$  is zero when the velocity  $V$  of the conductor is equal to the phase velocity of the wave. It is clear from (7.1.93) that under this synchronous condition there is no interaction between the conducting slab and the traveling current sheet. No currents are induced and the flux density completely penetrates the medium, with the characteristic exponential decay found in free space (Fig. 7.1.19). This figure shows how finite values of  $S$  give rise to currents that tend to exclude the magnetic flux density from the conductor. As  $S$  approaches infinity, the magnetic field is completely excluded from the conductor by a current density that is confined to a region very near the lower surface of the conductor. This is as would be expected, for, when  $V = 0$ , it is similar to the skin effect described in Section 7.1.3a. Here, however, the fields can also be excluded from the conductor because of the motion through a nonuniform field. To illustrate this point suppose that the current sheet is stationary so that  $\omega = 0$ . Then  $S$  is proportional to the velocity  $V$ , and it is apparent that a large material velocity leads to a shielding of the fields from the conductor. Note that in this limit  $S$  is a magnetic Reynolds number based on the wavelength of the current sheet. Once again a large magnetic Reynolds number indicates that induced field effects are significant.

The currents induced in the conducting slab give rise to time average forces

in the  $y$ - and  $z$ -directions. Both forces are significant because they are basic to a number of practical applications. The force in the  $y$ -direction makes it possible to support or levitate the slab on the magnetic field, whereas the force in the  $z$ -direction makes it possible to accelerate the slab in the  $z$ -direction.

It is a straightforward matter to compute these forces from the solutions we have obtained, since the force density in the material is  $\mathbf{F} = \mathbf{J} \times \mathbf{B}$ . The time average force  $\langle T_z \rangle$  in the  $z$ -direction (per unit  $x$ - $z$  area) is

$$\langle T_z \rangle = \int_0^\infty \langle F_z \rangle dy, \quad (7.1.94)$$

where\*

$$\langle F_z \rangle = \frac{1}{2} \operatorname{Re} (\mathcal{J}_x \hat{B}_y^*)$$

with  $\hat{B}_y^*$  the complex conjugate of  $\hat{B}_y$ . The solutions of (7.1.91) and (7.1.93) make it possible to carry out the integration of (7.1.94) to obtain

$$\langle T_z \rangle = \frac{1}{4} \frac{\mu_0 K^2 S}{\sqrt{1+S^2} \operatorname{Re} \sqrt{1+jS}}. \quad (7.1.95)$$

As expected, when the currents are not induced in the slab ( $S = 0$ ) there is no force in the  $z$ -direction. It is significant that the sign of the  $z$ -directed force depends on the sign of  $S$ . If  $S$  is positive (the traveling wave has a phase velocity that exceeds  $V$ ), the traveling wave interaction tends to pull the slab in the  $z$ -direction. Conversely, if the phase velocity is slower than that of the slab, the induced currents tend to retard the motion of the slab. These properties are similar to those discussed for the induction machine in Section 4.1.6b. In fact, this interaction is the basis for a distributed linear induction machine.

The dependence of the time average force  $\langle T_z \rangle$  on the parameter  $S$  is shown in Fig. 7.1.20. Here it is apparent that there is an optimum value of  $S$  at which the maximum force per unit area  $\langle T_z \rangle$  is produced.† This maximum exists between low values of  $S$ , in which little current is induced in the medium, and large values of  $S$  in which the induced currents have the wrong phase relationship with respect to the imposed current sheet to produce maximum force. Compare this discussion and Fig. 7.1.20 with Fig. 4.1.20 and the associated discussion for an induction machine. There is a direct correspondence between the parameter  $S$  used here and the slip  $s$  used in the induction-machine analysis. The physical phenomena that govern the shape of the force (or torque) as a function of  $S$  (or slip  $s$ ) are the same.

\* Here we use the identity  $\langle \operatorname{Re} \hat{A} e^{j\omega t} \operatorname{Re} \hat{B} e^{j\omega t} \rangle \equiv \frac{1}{2} \operatorname{Re} \hat{A} \hat{B}^*$ .

† This phenomenon is also used to achieve desired characteristics in deep-bar rotors of induction machines as discussed in Fitzgerald and Kingsley, *op. cit.*, p. 411.

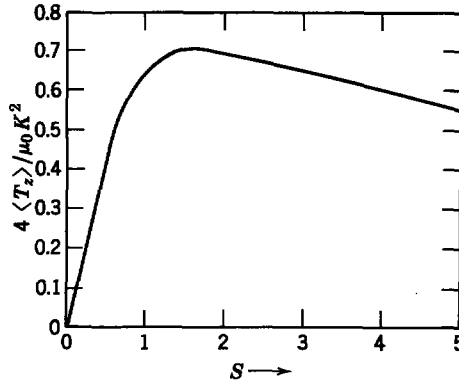


Fig. 7.1.20 Normalized time average force  $\langle T_x \rangle$  per unit  $x$ - $z$  area on the conducting slab of Fig. 7.1.18;  $S$  is defined following (7.1.87).

The time-average force density in the vertical ( $y$ )-direction is

$$\langle F_y \rangle = \frac{1}{2} \operatorname{Re} (\hat{J}_x \hat{B}_z^*) \quad (7.1.96)$$

The force per unit  $x$ - $z$  area  $\langle T_y \rangle$  can be computed in a manner similar to that used to find (7.1.95):

$$\langle T_y \rangle = \frac{\mu_0 K^2}{4} \left( \frac{\sqrt{1 + S^2} - 1}{\sqrt{1 + S^2}} \right) \quad (7.1.97)$$

The dependence of this levitating force on  $S$  is shown in Fig. 7.1.21. As  $S$  is increased, the upward force approaches an asymptotic value of  $\mu_0 K^2/4$ . As discussed in Chapter 8, this is the average magnetic pressure that acts on a perfectly conducting surface. A levitation experiment is shown in Fig. 7.1.22.

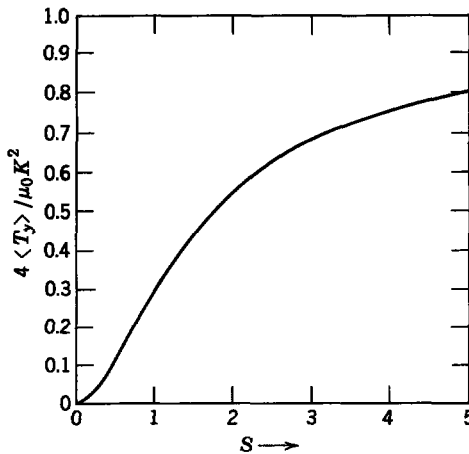
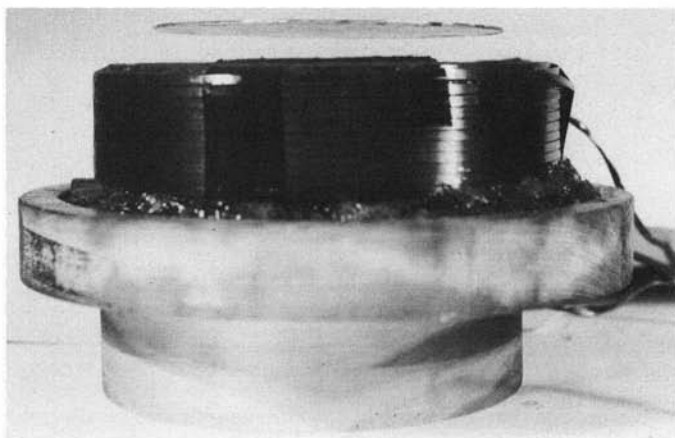


Fig. 7.1.21 Normalized time average force  $\langle T_y \rangle$  per unit  $x$ - $z$  area.



**Fig. 7.1.22** Laboratory project in which an aluminum disk (about 6 in. in diameter) is levitated by an alternating magnetic field. The coil is driven by a 400-Hz current. The experiment demonstrates qualitatively the induced force given by (7.1.97) with  $V = 0$ . Of course, in the experiment the finite thickness of the disk is highly significant (see Fig. 7.1.15) with  $\sigma = 3.7 \times 10^7$  mhos/m.

## 7.2 CHARGE RELAXATION

As discussed in the introduction to this chapter, the relaxation of charge in slightly conducting media constitutes the mechanism by which motion has an effect on electric field distributions in electric field systems. This is illustrated in the following sections by a series of examples. First, the relaxation of charge in systems involving media at rest is considered. Here the relaxation time is of fundamental importance in determining volume and surface charge densities that result from initial conditions and from excitations. In Section 7.2.2 emphasis is given to the effect of steady motion on the relaxation of free charge. In this case the electric Reynolds number based on the material velocity is important. Sections 7.2.3 and 7.2.4 then consider systems in which relaxation is affected by two characteristic times, a time that characterizes an electrical excitation and a time based on the material velocity and characteristic length.

The field equations for an electric field system (see Table 1.2)\* are

$$\nabla \times \mathbf{E} = 0, \quad (7.2.1)$$

$$\nabla \cdot \epsilon \mathbf{E} = \rho_f, \quad (7.2.2)$$

$$\nabla \cdot \mathbf{J}_f + \frac{\partial \rho_f}{\partial t} = 0 \quad (7.2.3)$$

where we have assumed  $\mathbf{D} = \epsilon \mathbf{E}$ .

\* See Appendix E.

In this section we confine our attention to situations in which the conduction of free charge can be accounted for by a constitutive law in the form

$$\mathbf{J}_f = \sigma \mathbf{E} + \rho_f \mathbf{v}. \quad (7.2.4)$$

Here we have combined Ohm's law  $\mathbf{J}'_f = \sigma \mathbf{E}'$  with the field transformations  $\mathbf{E}' = \mathbf{E}$  and  $\mathbf{J}'_f = \mathbf{J}_f - \rho_f \mathbf{v}$ .<sup>\*</sup> This law describes the conduction process in a wide range of solids, liquids, and gases but is by no means of general applicability.

There is a considerable analogy between the way in which we develop the subject of charge relaxation in this section and the way in which magnetic diffusion is developed in Section 7.1; for example, we begin by developing an equation that, together with appropriate boundary conditions, defines the distribution of the electric field, given the velocity of the medium.<sup>†</sup> From (7.2.3) and (7.2.4)

$$\nabla \cdot \sigma \mathbf{E} + \nabla \cdot \rho_f \mathbf{v} + \frac{\partial \rho_f}{\partial t} = 0. \quad (7.2.5)$$

The free charge density  $\rho_f$  can be eliminated from this expression by using (7.2.2).

$$\nabla \cdot \sigma \mathbf{E} + \nabla \cdot (\mathbf{v} \nabla \cdot \epsilon \mathbf{E}) + \frac{\partial}{\partial t} \nabla \cdot \epsilon \mathbf{E} = 0. \quad (7.2.6)$$

Given the velocity  $\mathbf{v}$ , this expression involves only the electric field intensity  $\mathbf{E}$ . It is a scalar equation, hence does not in general define the three components of  $\mathbf{E}$ . From (7.2.1), however, we can define a potential  $\phi$  such that

$$\mathbf{E} = -\nabla \phi. \quad (7.2.7)$$

Then (7.2.6) becomes one equation in one unknown.

$$\nabla \cdot \sigma \nabla \phi + \nabla \cdot (\mathbf{v} \nabla \cdot \epsilon \nabla \phi) = -\frac{\partial}{\partial t} \nabla \cdot \epsilon \nabla \phi. \quad (7.2.8)$$

Physically, this equation accounts for the conservation of free charge. The first term accounts for the flow of free charges into a small volume due to conduction. The second term appears because convection of the medium can give rise to the transport of free charge into a given region. Then the term on the right is the rate of increase of the local free charge density. Equation 7.2.8 serves the same purpose in a distributed electric field system as the electrical equation of motion served in the lumped-parameter descriptions of Chapters 2 to 5. In the sections that follow we confine our attention to the effect of the motion (if there is motion) on the fields; that is, the velocity  $\mathbf{v}$  is prescribed. One objective is an indication of models that can

<sup>\*</sup> Table 6.1, Appendix E.

<sup>†</sup> In the development of this section  $\sigma$  and  $\epsilon$  are assumed to be given functions of the space coordinates.

be used to simplify the analysis of electromechanical coupling, in which the velocity  $\mathbf{v}$  is not known until the fields are known.

### 7.2.1 Charge Relaxation as an Electrical Transient

We first consider the relaxation of charge in the absence of motion. A common situation is one in which the conductivity  $\sigma$  and permittivity  $\epsilon$  of each medium are uniform; thus changes in conductivity and permittivity occur only at surfaces. In these important situations it is essential to recognize that in the absence of a free charge source in the medium there will be no steady-state volume free-charge density. This is one of the important points to be made in the following subsection.

#### 7.2.1a Media with Uniform Properties

Suppose that we are concerned with the free-charge density in a medium at rest. Then the second term in (7.2.8) is zero and (7.2.2) and (7.2.7) can be used to write this expression as

$$\frac{\partial \rho_f}{\partial t} + \frac{\sigma}{\epsilon} \rho_f = 0. \quad (7.2.9)$$

A more direct derivation of this equation simply combines (7.2.2) to (7.2.4) with  $\mathbf{v} = 0$ . A general solution to (7.2.9) is

$$\rho_f(x, y, z, t) = \rho_0(x, y, z)e^{-(\sigma/\epsilon)t}, \quad (7.2.10)$$

as can be seen by substitution into (7.2.9); that is, given an initial free-charge distribution  $\rho_0$  at  $t = 0$ , the free charge density at each point in space decays to zero with the *relaxation time*  $\tau$ .

$$\tau = \frac{\epsilon}{\sigma}. \quad (7.2.11)$$

Unless there are sources of free charge in the volume of the material [which would contribute a driving term to (7.2.9)], there are no steady-state charges in the bulk. Note that (7.2.9) can be derived without recourse to (7.2.1), so that these conclusions do not depend on the field equations being quasi-static. Of course, in any physical situation the uniformly conducting medium is of finite extent and conservation of charge requires that those charges initially distributed throughout the volume relax to the surfaces that bound the volume. This can best be shown by means of an example.

**Example 7.2.1.** A conducting shell contains a uniformly conducting sphere at its center (Fig. 7.2.1). The region between the sphere and the shell is perfectly insulating. At time  $t = 0$  there is a free charge density  $\rho_0$  distributed uniformly throughout a spherical region of radius  $R$  at the center of the conducting sphere; that is, if we call the total charge supported by the center sphere  $Q$ ,

$$\rho_f(r < R, t = 0) = \rho_0 = Q/(4/3)\pi R^3. \quad (a)$$

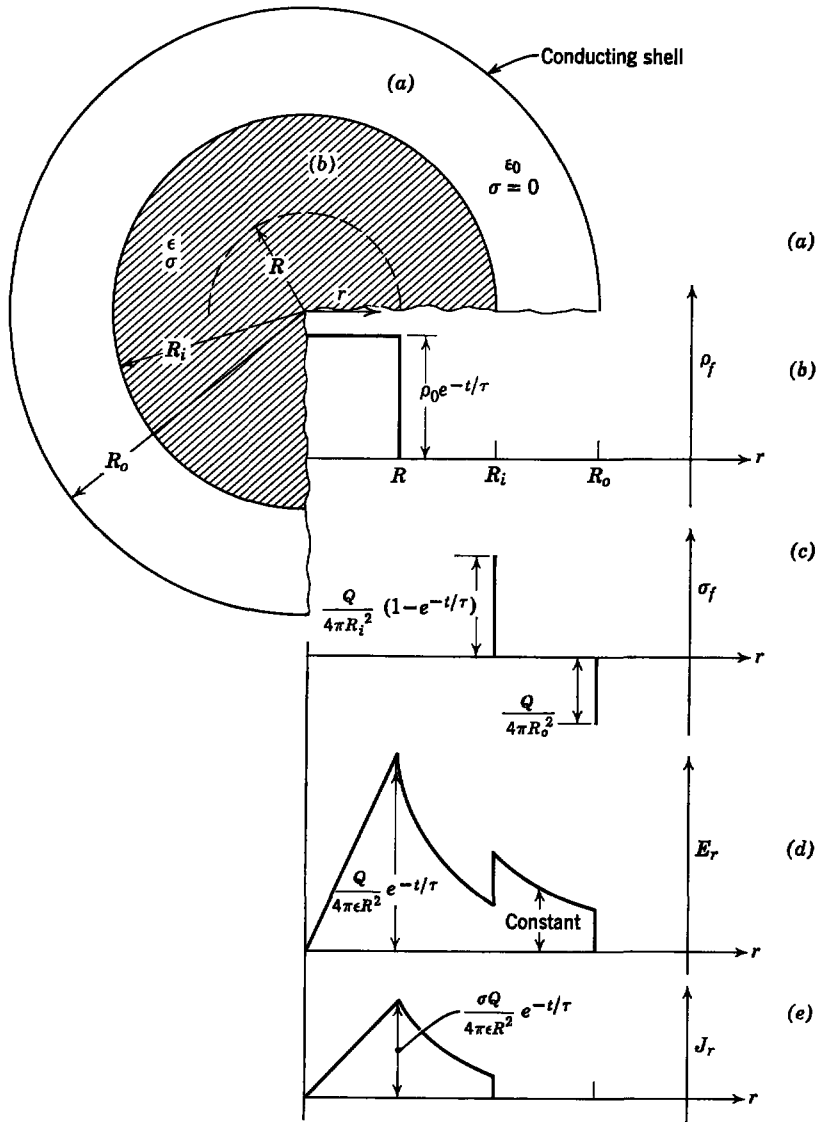


**Fig. 7.2.1** (a) A uniformly conducting sphere of radius  $R_i$  is bounded by an insulating medium and a perfectly conducting shell of radius  $R_o$ ; (b) when  $t = 0$ , the sphere supports a volume charge distributed uniformly over the region  $r < R$ ; (c) for  $t > 0$  charges accumulate at  $r = R_i$ ; (d) radial electric field  $E_r$ ; (e) current density  $J_r$ .

The transient charge density follows from (7.2.10)

$$\begin{aligned} \rho_f &= \rho_0 e^{-t/\tau} & \text{for } r < R, \\ \rho_f &= 0 & \text{for } r > R. \end{aligned} \quad (b)$$

This distribution of volume charge density is shown in Fig. 7.2.1b.

The problem has radial symmetry. Hence the charge distribution of (b) can be used with (7.2.2) to determine the radial component of the electric field intensity since

$$\frac{1}{r^2} \frac{d}{dr} (r^2 E_r) = \frac{\rho_0}{\epsilon} e^{-t/\tau}. \quad (c)$$

This expression can be integrated to obtain

$$E_r^b = \frac{Q}{4\pi\epsilon R^2} \left(\frac{r}{R}\right) e^{-t/\tau}; \quad r < R \quad (d)$$

The total charge within the radius  $r = R$  is  $Qe^{-t/\tau}$ . Then the integral form of Gauss's theorem shows that

$$E_r^b = \frac{Q}{4\pi\epsilon r^2} e^{-t/\tau}; \quad R < r < R_i \quad (e)$$

Similarly, since the total charge on the sphere must be conserved, the electric field outside the conducting sphere is

$$E_r^a = \frac{Q}{4\pi\epsilon_0 r^2}; \quad R_i < r < R_o \quad (f)$$

These last two electric field intensities can be used to determine the amount of free charge on the surface of the inner sphere, since

$$\sigma_f = \epsilon_0 E_r^a (r = R_i) - \epsilon E_r^b (r = R_i) = \frac{Q}{4\pi R_i^2} (1 - e^{-t/\tau}). \quad (g)$$

Of course, the surface charge on the outer shell is constant, for the electric field in the insulating section adjacent to the shell is constant. The surface charge density and distribution of  $E_r$  are shown in Fig. 7.2.1c,d. It is clear from the solutions that the initial free-charge density relaxes to the outer surface of the conducting sphere. In the steady-state condition there is no electric field within the sphere, but rather the field is shielded out of the sphere by the surface charge at  $r = R_i$ .

Remember that the current density is

$$J_r = \sigma E_r \quad (h)$$

and is therefore distributed as shown in Fig. 7.2.1e. It is this current that accounts for the conduction of free charge to the surface of the sphere. Note that there is a conduction current in the region  $R < r < R_i$ , even though at no time during the transient is there a free-charge density in this region. Conduction currents modeled by a constitutive law in the form of (7.2.4) can be present in a medium in the absence of  $\rho_f$ .

Without injection of charges directly into the bulk of the material, a uniformly conducting medium with uniform permittivity does not support a volume charge density as illustrated by Example 7.2.1. In such systems free charges are confined to surfaces. These surface charges can relax through a

medium and this surface-charge relaxation is accounted for through boundary conditions. Lumped-parameter models often can be used to represent this process, as illustrated by the following example.

**Example 7.2.2.** The important role of surface-charge relaxation through dielectrics can be demonstrated by means of the experiment shown in Fig. 7.2.2. Three plane parallel metallic electrodes are immersed in a liquid dielectric as shown. A voltage source  $V_o$  is used to establish a positive charge on the middle electrode. At time  $t = 0$  the switch  $S$  connects the battery to the terminal (2), leaving the middle plate isolated from the other two plates except for conduction through the dielectric. We wish to compute the electric fields defined in Fig. 7.2.2 as functions of time, to show the relaxation of charge from the middle plate.

We assume that the fields are uniformly distributed between the plates so that for  $t < 0$

$$E_a = \frac{V_o}{a}, \tag{a}$$

$$E_b = 0. \tag{b}$$

We integrate the conservation of charge equation (7.2.3) over the volume that encloses the middle plate to write

$$(J_a - J_b) = -\frac{\partial}{\partial t} \epsilon(E_a - E_b). \tag{c}$$

This equation guarantees that the rate of change of charge on the middle plate is accounted for by current to either of the other plates. The current densities can be replaced by the

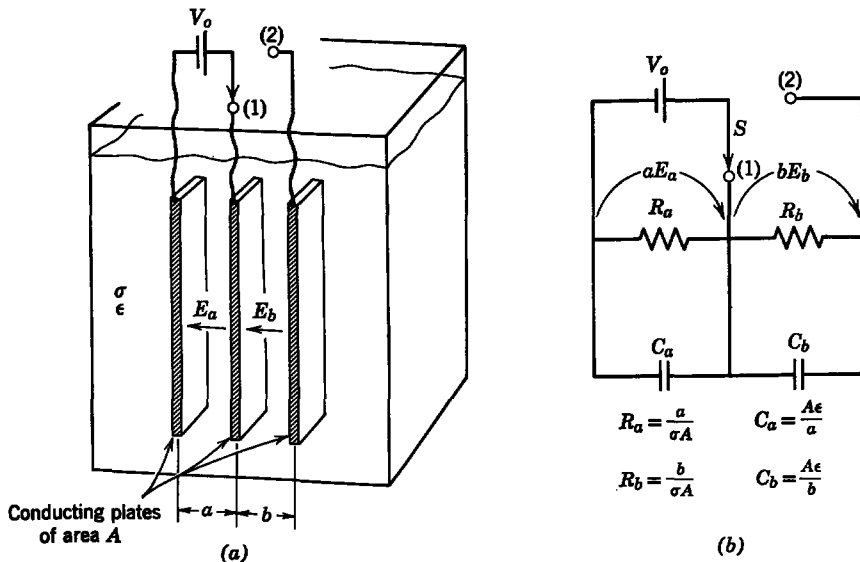


**Fig. 7.2.2** System of three parallel-plane metallic electrodes immersed in a dielectric of conductivity  $\sigma$  and permittivity  $\epsilon$ : at  $t = 0$  the switch is connected to terminal (2); (b) equivalent circuit.

electric field intensities by using (7.2.4) with  $v = 0$ :

$$\sigma(E_a - E_b) = -\frac{d}{dt} \epsilon(E_a - E_b). \quad (d)$$

This expression is recognized as having the same form as (7.2.9) except that the charge density is replaced by the jump in electric field intensity, which is proportional to the charge density on the middle plate. If we use the initial conditions of (a) and (b) the solution to (d) is

$$E_a - E_b = \frac{V_o}{a} e^{-t/\tau}; \quad \tau = \frac{\epsilon}{\sigma}. \quad (e)$$

For  $t > 0$  the voltage across the outside plates is constrained to be  $V_o$ , hence

$$E_a a + E_b b = V_o. \quad (f)$$

We solve for both  $E_a$  and  $E_b$  from these last two equations.

$$E_a = \frac{V_o}{a+b} \left( 1 + \frac{b}{a} e^{-t/\tau} \right), \quad (g)$$

$$E_b = \frac{V_o}{a+b} (1 - e^{-t/\tau}). \quad (h)$$

These solutions are shown in Fig. 7.2.3. Initially, all of the charge is retained on the middle plate. [Recall that the charge on the middle plate is at first  $(A\epsilon V_o/a)$  and is always  $A\epsilon(E_a - E_b)$ .] All the charge relaxes to the outer plates with the characteristic relaxation time  $\tau$ . The relaxation of charge is a fundamental way of viewing the decay of the  $RC$  circuit shown in Fig. 7.2.2. The solution using this circuit with the equivalent parameter values is the same as the solution just given for the continuum model. This example provides the answer to the question posed in Fig. 7.2.4.

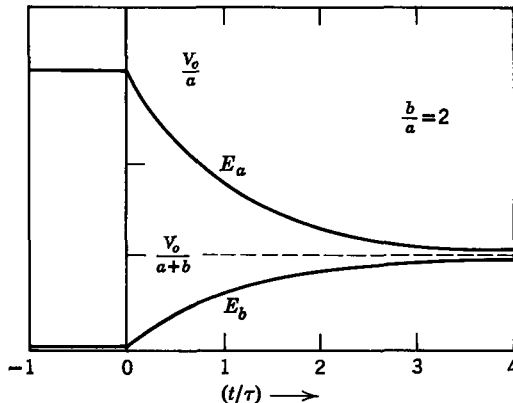


**Fig. 7.2.3** Relaxation of the electric field intensities between the plates in Fig. 7.2.2 when  $S$  is switched from (1) to (2). The surface charge density on the middle plate is proportional to the difference between  $E_a$  and  $E_b$ .

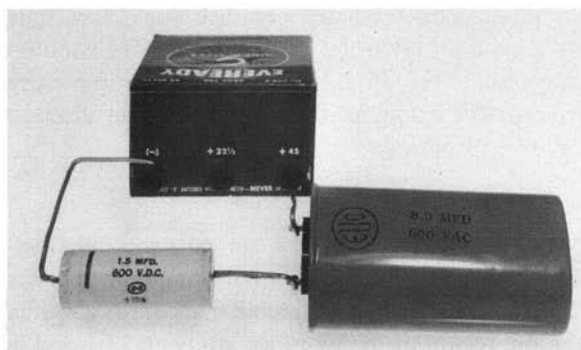


**Fig. 7.2.4** The capacitors are connected in series with the battery. The circuit has been completed for a sufficient length of time to establish steady-state conditions. Why is it not possible, on the basis of the given information, to determine the steady-state charge stored in each of the capacitors? (See Example 7.2.2.)

Whether we are concerned with relaxation of charge from the bulk or from an interface, the relaxation time  $\epsilon/\sigma$  is of fundamental importance. In Table 7.2.1 we see that the relaxation time depends greatly on the material used. In metals the volume distribution of charge would be difficult to measure, let alone ever be large enough to include in a physical model. On the other hand, there are many materials in which the relaxation time can be measured in minutes or even hours. In slightly conducting materials, however, the conductivity is often extremely sensitive to impurities and sources of

**Table 7.2.1** Characteristic Values of Relaxation Time  $\tau = \epsilon/\sigma$  for Conductors and Insulators

Material	$\sigma$ (mhos/meter)	$\epsilon$	$\tau$ (sec)
Silver*	$6.17 \times 10^7$	$\epsilon_0$	$1.43 \times 10^{-19}$
Copper*	$5.80 \times 10^7$	$\epsilon_0$	$1.52 \times 10^{-19}$
Aluminum*	$3.72 \times 10^7$	$\epsilon_0$	$2.38 \times 10^{-19}$
Mercury†	$1.06 \times 10^6$	$\epsilon_0$	$8.35 \times 10^{-18}$
Seawater*	4	$80 \epsilon_0$	$1.77 \times 10^{-10}$
Water†	$4 \times 10^{-6}$	$80 \epsilon_0$	$1.77 \times 10^{-4}$
Nitrobenzene†	$5 \times 10^{-7}$	$36.1 \epsilon_0$	$6.40 \times 10^{-4}$
Corn oil	$5 \times 10^{-11}$	$2.7 \epsilon_0$	4.8
Carbon tetrachloride†	$4 \times 10^{-16}$	$2.24 \epsilon_0$	$4.95 \times 10^4$

\* S. Ramo, and J. R. Whinnery, *Fields and Waves in Modern Radio*, Wiley, New York, 1958, pp. 240 and 312.

† N. A. Lange, *Handbook of Chemistry*, Handbook Pub., Inc., Sandusky, Ohio, 1952, pp. 1240 and 1253.

ionization. For this reason tabulated conductivities, especially for liquids, are likely to indicate only the order of magnitude. We should bear in mind also that the constitutive law of (7.2.4) may be a poor approximation for the conduction process; for example, the mobility model discussed in Section 6.3.2 may be more appropriate.

### 7.2.1b Media with Nonuniform Properties

A steady-state volume charge density can exist in a medium at rest when there are gradients of either the conductivity or permittivity in the bulk of the material. The interface between dissimilar media is a special case of this situation, for in the region of the interface gradients of  $\epsilon$  and  $\sigma$  are singular. It is for this reason that surface charges accumulate on the surfaces of uniformly conducting media.

With  $\sigma$  and  $\epsilon$  functions of position the potential in a stationary medium must satisfy the expression

$$\nabla \cdot \sigma \nabla \phi + \frac{\partial}{\partial t} \nabla \cdot \epsilon \nabla \phi = 0, \quad (7.2.12)$$

as we can see from (7.2.8). Note that this expression does not take the simple form of (7.2.9) unless  $\sigma$  and  $\epsilon$  are constant. A one-dimensional example serves to illustrate the consequences of nonuniform properties in electric field systems.

**Example 7.2.3.** Plane parallel electrodes bound a material of nonuniform properties shown in Fig. 7.2.5. For purposes of illustration we consider the case in which an external current source drives a current through the material in the  $x$ -direction. The material properties depend only on the  $x$ -dimension. We wish to determine the free charge density and distribution of electric field intensity between the plates. Physically, this situation would be realized by simply placing electrodes with a temperature difference in an organic liquid. The conductivity is a strong function of temperature in many liquids and there would therefore be a variation in  $\sigma$  as a function of  $x$ .

In one dimension the gradient of  $\phi$  in (7.2.12) becomes  $(-E_x)$ ; hence (7.2.12) can be written as

$$\frac{\partial}{\partial x} \left[ \frac{\partial}{\partial t} (\epsilon E_x) + \sigma E_x \right] = 0. \quad (a)$$

This expression can be integrated to obtain

$$\frac{\partial}{\partial t} (\epsilon E_x) + \sigma E_x = f(t). \quad (b)$$

This result is not surprising, for it simply states that the sum of the displacement and conduction currents passing any given  $y$ - $z$  plane is the same as that found at any other  $y$ - $z$  plane; That is,  $f(t)$  is simply the current density  $i(t)/A$ :

$$\frac{\partial}{\partial t} (\epsilon E_x) + \sigma E_x = \frac{i(t)}{A}. \quad (c)$$

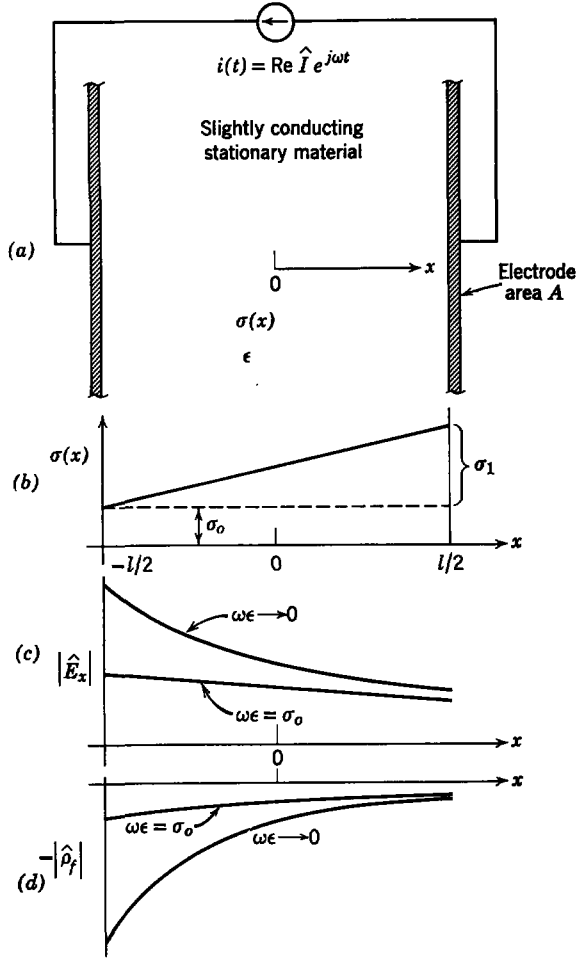


**Fig. 7.2.5** (a) A slightly conducting material of uniform permittivity is bounded by plane-parallel electrodes of area  $A$ ; (b) conductivity distribution between plates; (c) distribution of the electric field magnitude; (d) free charge density magnitude.

To emphasize the fact that under steady-state conditions there are bulk charges in the nonuniform medium consider a sinusoidal driving current

$$i(t) = \text{Re} (\hat{I} e^{j\omega t}), \tag{d}$$

hence sinusoidal responses in the form

$$E_x = \text{Re} [\hat{E}_x(x) e^{j\omega t}]. \tag{e}$$

Then substitution into (c) shows that

$$\hat{E}_x = \frac{\hat{I}}{A(j\omega\epsilon + \sigma)}. \tag{f}$$

Here  $\sigma$  and  $\epsilon$  are in general functions of  $x$ , hence so also is  $E_x$ . The charge density is found by using (7.2.2):

$$\hat{\rho}_f = \frac{d\epsilon \hat{E}_x}{dx} = -\frac{\epsilon \hat{I}}{A} \frac{[j\omega(d\epsilon/dx) + d\sigma/dx]}{(j\omega\epsilon + \sigma)^2} + \frac{\hat{I}(d\epsilon/dx)}{A(j\omega\epsilon + \sigma)}. \quad (g)$$

As a more particular example consider the case in which the conductivity has the linear distribution shown in Fig. 7.2.5*b* and the permittivity is constant.

$$\sigma(x) = \sigma_0 + \frac{\sigma_1}{l}x. \quad (h)$$

Then it follows from (f) and (g) that

$$|\hat{E}_x| = \frac{|\hat{I}|}{A\sqrt{\sigma^2 + (\omega\epsilon)^2}} \quad (i)$$

$$|\hat{\rho}_f| = \frac{\epsilon|\hat{I}| \sigma_1/A l}{[\sigma^2 + (\omega\epsilon)^2]}. \quad (j)$$

The distribution of electric field intensity and charge density magnitudes between the plates is shown in Fig. 7.2.5*c, d*. Note that the greatest amount of free charge exists in the bulk of the medium when the frequency is zero (the current is constant). The charge density tends to zero as the frequency is made large compared with the local reciprocal of the relaxation time  $\epsilon/\sigma$ . In the high frequency limit one period of excitation is insufficient time for the free charge to accumulate in the bulk of the material.

Bulk charge accumulation due to nonuniform conductivity occurs in many practical situations; for example, in oil-insulated, high-voltage dc cables for the transmission of power a temperature gradient in the oil can make the conductivity vary markedly with position. A bulk charge accumulates; and, when the applied voltage is reversed, the bulk charge may cause overly high electrical stresses and insulation failure before it can relax to a new steady-state distribution.\*

## 7.2.2 Charge Relaxation in the Presence of Steady Motion

We are now in a position to undertake a study of the effects of material motion on charge relaxation. In the sections that follow interest is confined to systems in which changes in material properties occur at surfaces and can be accounted for by the boundary conditions. Then, because  $\sigma$  and  $\epsilon$  are constant in the bulk of the material, (7.2.8) can be written as

$$\frac{\sigma}{\epsilon} \rho_f + \nabla \cdot \rho_f \mathbf{v} + \frac{\partial \rho_f}{\partial t} = 0, \quad (7.2.13)$$

where use has been made of (7.2.2) and (7.2.7) to state this equation in terms of the free charge density.

A great deal can be said about the implications of (7.2.13) in the important case in which the media are *incompressible*. In such situations the material density remains constant and the net flux of material into a given region is

\* See, for example, K. Kojima, S. Tanaka, and K. Matsuura, "Potential Distribution in Dielectrics of Oil-Filled, D-C Cable," *Elec. Eng. Japan*, August 1964.

zero. By analogy with a similar condition on the magnetic flux density ( $\nabla \cdot \mathbf{B} = 0$ ) the condition that the material be incompressible is stated as

$$\nabla \cdot \mathbf{v} = 0. \quad (7.2.14)$$

(More is said about this equation in Chapter 12, in which incompressible fluids are discussed.)

Expansion of the second term in (7.2.13) gives

$$\nabla \cdot \rho_f \mathbf{v} = \mathbf{v} \cdot \nabla \rho_f + \rho_f (\nabla \cdot \mathbf{v}), \quad (7.2.15)$$

where, in view of (7.2.14), the last term is zero. Hence (7.2.13) can be written as

$$\frac{\sigma}{\epsilon} \rho_f + \frac{\partial \rho_f}{\partial t} + \mathbf{v} \cdot \nabla \rho_f = 0. \quad (7.2.16)$$

Written in this form, it is clear that (7.2.16) expresses the same relaxation conditions as (7.2.9) did for stationary media, except that now the charge relaxation occurs with respect to the frame of the moving medium; that is, the last two terms in (7.2.16) (the convective derivative) represent the time rate of change of  $\rho_f$  for an observer moving with the velocity  $\mathbf{v}$  of the material. Hence the material motion simply serves to transport the free charge as it relaxes with the time constant  $\epsilon/\sigma$ .

**Example 7.2.4.** The relaxation of an initial distribution of charge placed in the fluid stream shown in Fig. 7.2.6 is to be considered. Note that the velocity  $\mathbf{v} = v_x(y)\mathbf{i}_x$  satisfies (7.2.14).

Remember that (7.2.16), which must be satisfied by the distribution of  $\rho_f$ , expresses the same relaxation phenomenon as (7.2.9), except that the relaxation occurs with respect to the moving medium. Hence we look for a solution to (7.2.16) that has the form of (7.2.10), with  $x$  replaced by  $x'$ , where

$$x' = x - v_x(y)t. \quad (a)$$

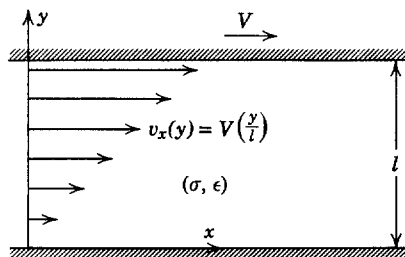


**Fig. 7.2.6** A fluid with uniform conductivity and permittivity is confined by parallel plates, one of which is fixed as the other moves to the right with the velocity  $V$ . The fluid, which then moves to the right with the velocity profile shown, is given an initial charge distribution which relaxes as shown in Fig. 7.2.7.

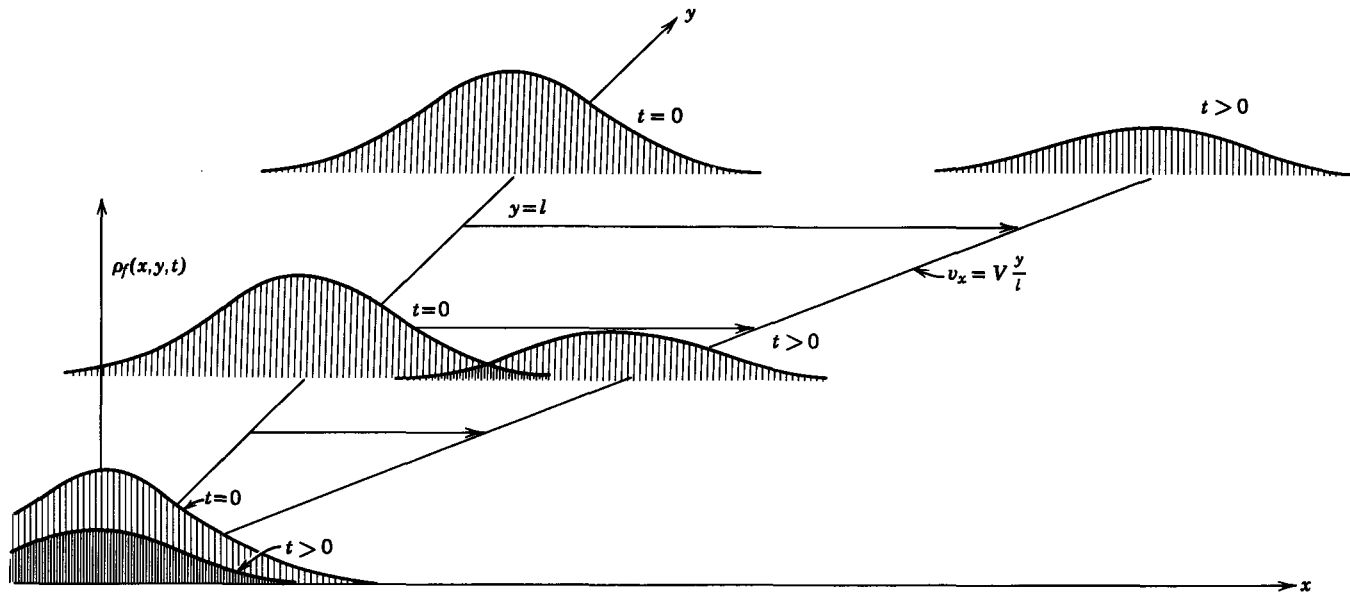


Fig. 7.2.7 An initial distribution of charge is transported downstream with the material velocity as it relaxes with the time constant  $\epsilon/\sigma$ .

By this reasoning the desired solution to (7.2.16) is

$$\rho_f = \rho_0[x - v_x(y)t, y]e^{-(\sigma/\epsilon)t}, \quad (b)$$

which can be checked by direct substitution. From this result it is clear that an initial charge distribution is simply translated downstream, attenuating in amplitude with the relaxation time  $\epsilon/\sigma$  but otherwise retaining its initial shape; for example, if at  $t = 0$  the charge distribution is

$$\rho_f(x, y, t = 0) = \rho_0 e^{-(x/l)^2}, \quad (c)$$

as shown in Fig. 7.2.7, the subsequent charge distribution will be

$$\rho_f(x, y, t) = \rho_0 \exp \left\{ - \left[ \frac{x - v_x(y)t}{l} \right]^2 \right\} e^{-(\sigma/\epsilon)t}. \quad (d)$$

This redistribution of the charge is also shown in Fig. 7.2.7. It is important to see that even in the presence of convection the steady-state charge density in source-free media with uniform electrical properties tends to zero.

It must be recognized that there is an electric potential associated with the charge density defined by (7.2.16). In the simple bulk relaxation problem considered here it is possible to determine the charge density without recourse to the boundary conditions, hence to the potential  $\phi$ . Many practical devices exploit the energy conversion process that takes place when the charge is transported from a region of one potential to a region of another. To determine whether energy is taken from the moving medium (a generator) or put into the medium (motor or pump) it is necessary to know the potential distribution. A simple illustration of this kind of problem is made next. The conditions required within the medium for appreciable charge transport are apparent from the developments of this section. The time required for a given initial distribution of charge to relax (with respect to the medium) is  $\epsilon/\sigma$ , whereas the time required for the transport of the charge over a distance  $l$  with the velocity  $V$  is  $l/V$ . For an appreciable convection of charge the transport time must be short compared with the relaxation time; that is

$$R_e = \frac{\epsilon/\sigma}{l/V} = \frac{\epsilon V}{\sigma l} \gg 1 \quad (7.2.17)$$

or the electric Reynolds number  $R_e$  must be large compared with one if the convection is to compete with the relaxation process in determining the location of the volume charge density.

One highly developed application of the ideas introduced in this section is to the generation of extremely high voltages. Here the basic electro-mechanical system is a Van de Graaff generator that uses the mechanical motion of an insulator to transport free charge against an electric field and generate high-voltage dc power.\* A simple model for this generator is the subject of the following example.

\* A description of this and other sources of power is given in J. G. Trump, "Electrostatic Sources of Electric Power," *Elec. Eng.*, June 1947.

**Example 7.2.5.** The basic system, illustrated in Fig. 7.2.8a, consists of a continuous belt made of slightly conducting material, which is driven by rollers at the constant velocity

$$\mathbf{v} = \mathbf{i}_z V.$$

The electrode at  $z = 0$  feeds positive ions onto the surface of the belt and the electrode at  $z = l$  removes the positive ions. The two electrodes are the electrical terminals that will remain open-circuited for this example. The belt material has a constant conductivity  $\sigma$  and constant permittivity  $\epsilon$  but the positive ions put on the belt by the electrode are immobile.

The analysis of the system begins with the following assumptions:

1. We consider only that portion of the belt that carries charge from  $z = 0$  to  $z = l$ .
2. The electric field intensity and current density have only  $z$  components:

$$\mathbf{E} = \mathbf{i}_z E,$$

$$\mathbf{J}_f = \mathbf{i}_z J.$$

3. All variables are functions of  $z$  alone.
4. In the spirit of the one-dimensional model we assume that the net effect of the positive ions applied to the belt and the induced charge in the belt can be represented by an effective free charge density  $\rho_f$  which is a function of  $z$  only.
5. We assume that the electrode at  $z = 0$  maintains the boundary condition

$$\text{at } z = 0, \quad \rho_f = \rho_0. \quad (\text{a})$$

6. The system is operating in the steady state.

With the conductivity constant, the constituent relation for the transport of free charge is (7.2.4)

$$J = \sigma E + \rho_f V. \quad (\text{b})$$

The other equations necessary for the analysis are Gauss's law (7.2.2) written as

$$\epsilon \frac{dE}{dz} = \rho_f \quad (\text{c})$$

and the condition imposed by the open circuit

$$J = 0. \quad (\text{d})$$

We differentiate (b) with respect to  $z$  and use (c) to eliminate  $E$  and obtain

$$V \frac{d\rho_f}{dz} + \frac{\sigma}{\epsilon} \rho_f = 0. \quad (\text{e})$$

The general solution of this equation is

$$\rho_f = C_1 e^{-\sigma z / \epsilon V}. \quad (\text{f})$$

We use boundary condition (a) to evaluate the constant  $C_1$  and obtain the solution

$$\rho_f = \rho_0 e^{-z/R_e l}; \quad R_e = \frac{\epsilon V}{\sigma l}. \quad (\text{g})$$

Finally, we calculate the open-circuit voltage by using (b) and (d):

$$V_{\text{oc}} = - \int_0^l E_z dz = R_e^2 \frac{\rho_0 l^2}{\epsilon} (1 - e^{-1/R_e}). \quad (\text{h})$$

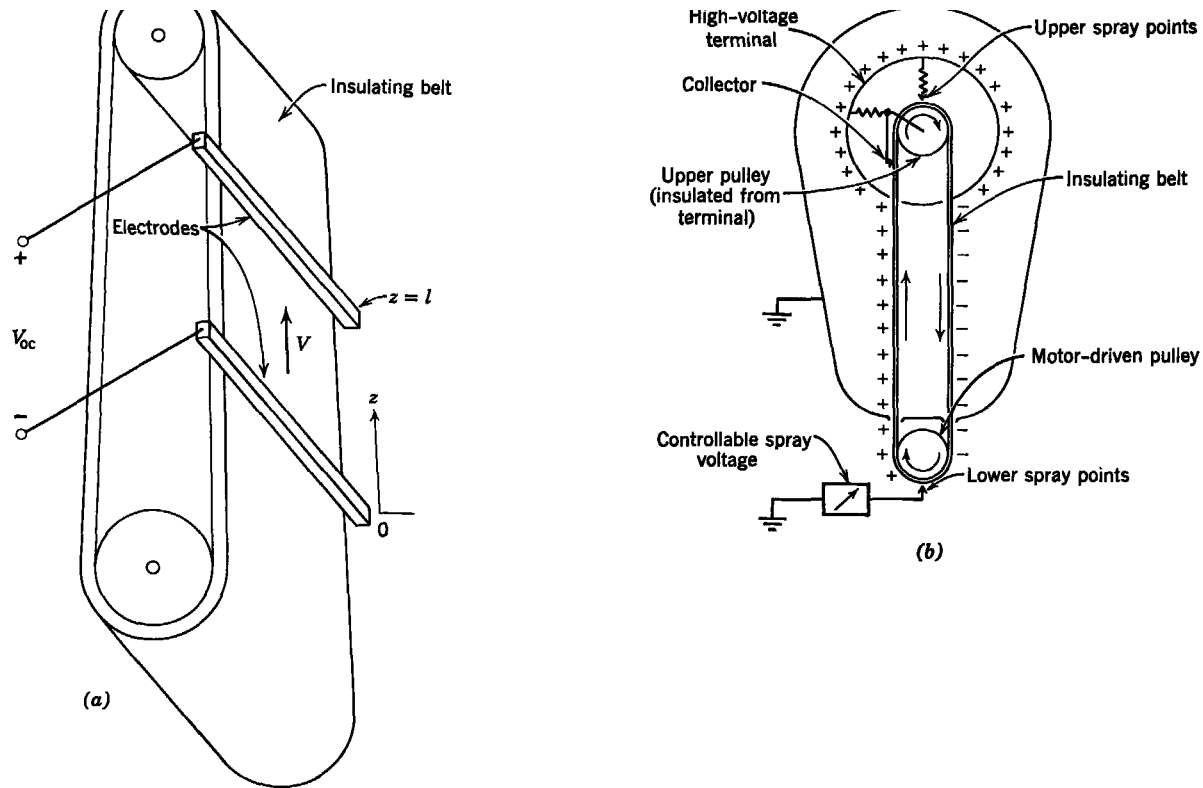


**Fig. 7.2.8** (a) A simple model for a Van de Graaff generator. Charges are conveyed to the belt at  $z = 0$  and transported in the presence of relaxation to the electrode at  $z = l$  through a potential difference  $V_{0c}$ . (b) A more realistic schematic diagram of the generator shows how the charge is injected and removed with corona sources. In a practical device the conduction along the belt does not represent a significant limitation.

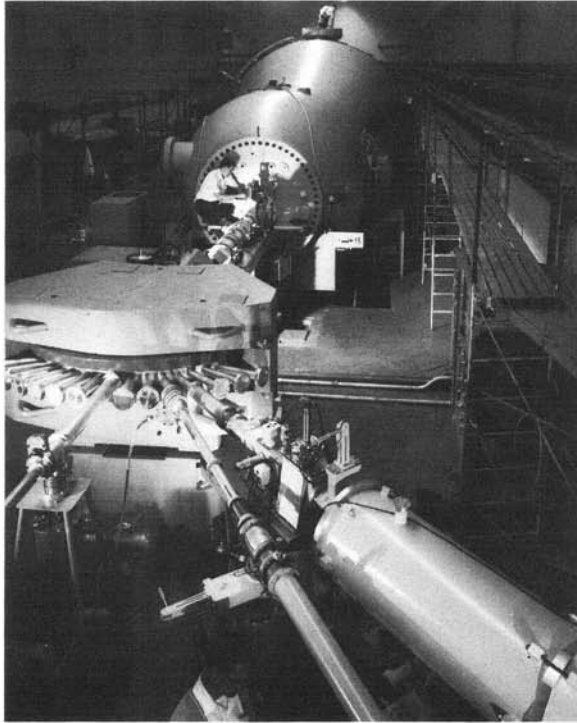


**Fig. 7.2.8c** Van de Graaff tandem accelerator at High Voltage Engineering Corporation, Burlington, Mass. Capable of a terminal potential of 10 MV, this machine weighs 188 tons, is 18 ft in diameter, and is 81 ft long.

The distributions of free charge density  $\rho_f$  and field intensity  $E$  along the belt are shown in Figs. 7.2.9 and 7.2.10. To interpret these curves, consider that  $\epsilon$  and  $l$  are fixed and that  $R_e$  is changed by varying  $\sigma$  and/or  $V$ . The current density  $J$ , as given by (b), indicates that free charge is transported by conduction ( $\sigma E$ ) and by convection ( $\rho_f V$ ). As indicated earlier in this section, the presence of conduction makes the free charge tend to relax to the surfaces of the conductor. Thus in this system we have two competing processes: (a) convection of the charge in the positive  $z$ -direction by the moving belt and (b) relaxation of free charge in the belt to neutralize the injected charge. It is apparent from the curves of Fig. 7.2.9 that the electric Reynolds number  $R_e$  is a measure of the relative effectiveness of these two processes. For a large  $R_e$  the relaxation process is relatively ineffective and the charge density varies very little along the length of the device. On the other hand, for small  $R_e$ , the relaxation process predominates and the net charge density decays rapidly along the length because induced charge can build up in the belt to neutralize the injected charge.

It is clear that because the amount of net free charge between the electrodes varies significantly with  $R_e$  so will the electric field intensity. As indicated by (b) and (d),  $E$  has the same space variation as the charge density but its magnitude is a function of  $R_e$  also.

For the three values of  $R_e$  for which curves are plotted in Figs. 7.2.9 and 7.2.10 we calculate the open-circuit voltage from (h) and give the values in Table 7.2.2.

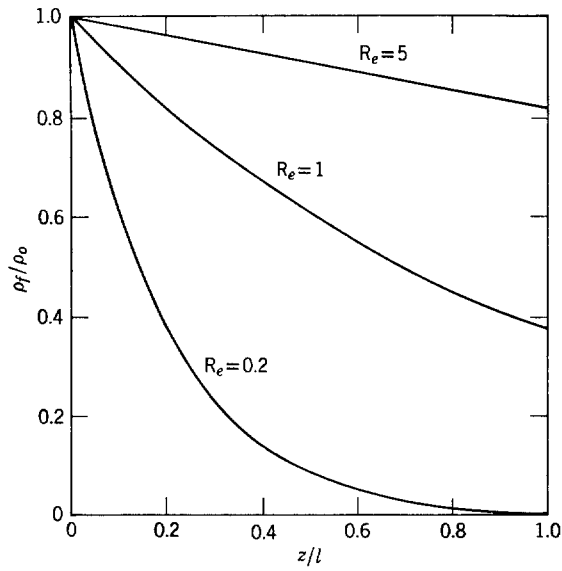


Fig. 7.2.9 Variation of net free charge density with position.

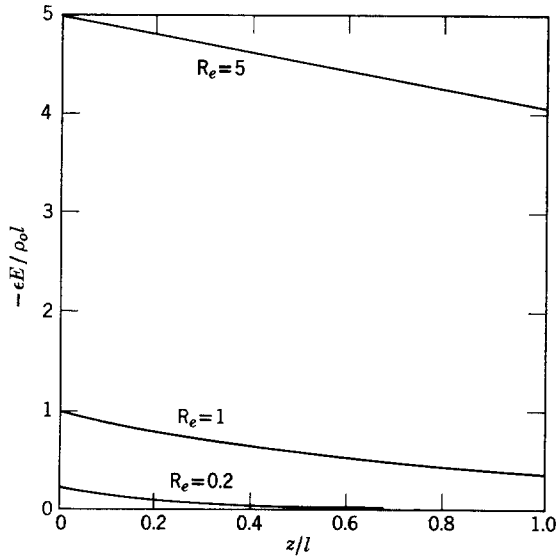


Fig. 7.2.10 Variation of electric field intensity with position.

Table 7.2.2

$R_e$	$\frac{\epsilon V_{oc}}{\rho_o l^2}$
0.2	0.0373
1.0	0.632
5.0	4.55

Thus for fixed geometry ( $l$ ), fixed charge density at  $z = 0(\rho_o)$ , and fixed permittivity the open-circuit voltage is increased by increasing the velocity ( $V$ ) of the belt or by decreasing the conductivity ( $\sigma$ ) of the belt material. In either case the electric Reynolds number is increased. Note from (h) that the open-circuit voltage increases in proportion to  $R_e$ . Thus for the highest possible open-circuit voltage we must make the velocity as high as possible and the conductivity as low as possible.

In the previous example, we assumed that the electric field intensity and material motion were in the same direction. Practical generators are shown in Figs. 7.2.8*b-c*. In these devices, the component of the electric field intensity due to charge on the belt (as compared to that on the terminals) is essentially perpendicular to the direction of motion, and hence a somewhat different model is appropriate for quantitative purposes.

For conceptual simplicity we have so far in this section emphasized the effect of material motion on electric fields in situations in which the material could be essentially characterized by a single electric Reynolds number. Cases in which electric fields interact with continuous media are extremely diverse, both in terms of the mechanism basic to the interaction and in terms of possible applications. This point can be illustrated by considering an example that has some of the basic ingredients of a thunderstorm. This is a system that involves a highly insulating gas (the air, with a relaxation time that can be measured in hours) and water drops (with a relaxation time considerably less than a millisecond). The experiment is an electrohydrodynamic dynamo, in that the motion of the liquid drops is responsible for the generation of extremely high voltages with no external electrical excitations.

**Example 7.2.6.** The experiment is shown in Fig. 7.2.11. It can be simply constructed from two cans, two pieces of wire, and a pair of pipettes connected to a container of water. Flow of water through the pipettes is adjusted so that the streams break up into drops in the vicinity of the conducting rings. These rings encircle the streams but do not make electrical contact with the drops. The rings are connected, respectively, to the opposite cans, as shown in Fig. 7.2.11. It is extremely important that these cans be carefully insulated from each other. This can be done, as shown in Fig. 7.2.11*a*, by supporting the cans on a dry piece of plastic.

With no external excitations, the apparatus shown in Fig. 7.2.11*a* is capable of producing 10 to 20 kV. This potential difference, which appears between the cans, can be measured with an electrostatic voltmeter, not shown in Fig. 7.2.11*a*.

The formulation of a quantitative model for this experiment affords an opportunity not only to illustrate further the effect on electric fields of media in motion but also to undertake the modeling process itself. In all the examples found in this chapter mathematical models were involved. Here we are involved with the experiment itself and must translate the

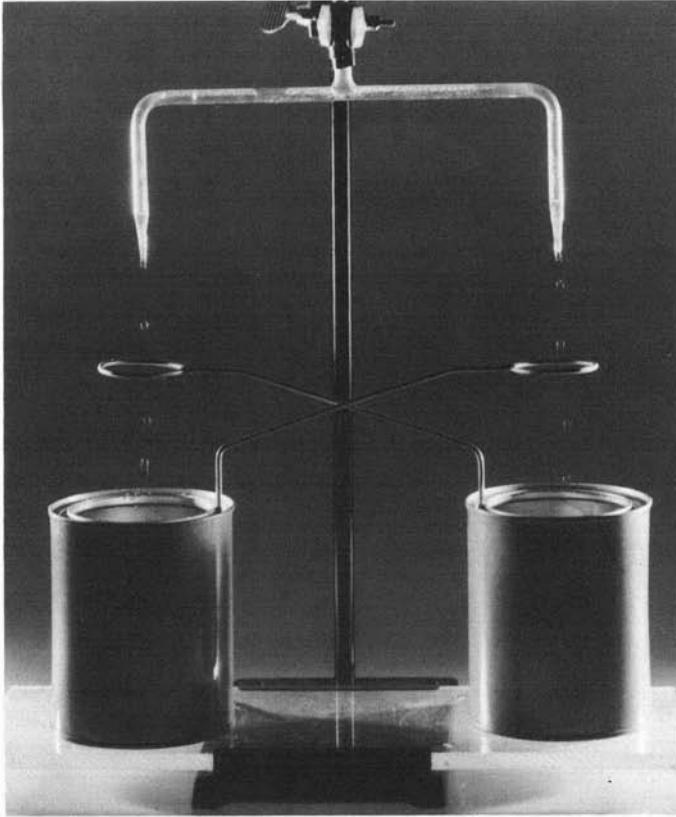


**Fig. 7.2.11a** Water drops fall into the cans through cross-connected wire loops. A potential difference of more than 20 kV between cans is spontaneously generated by the motion of the drops. For optimum operation the drops should form nearer to the rings than shown. This is accomplished by increasing the flow rate.

observed phenomena into a mathematical explanation. (Of course, actually envisioning the experiment is an even more demanding intellectual process for which we must credit Lord Kelvin.\*)

First of all we require a plausible explanation for the generated voltage. Suppose that at a given instant the left ring in Fig. 7.2.11b has a slight excess charge (either due to random fluctuations or to an initial charge purposely placed on the ring). Then charges of the opposite polarity will be induced on the stream passing through the ring, as shown in Fig. 7.2.12. This stream breaks up into drops in the region of the ring; and, as a result, the fully formed drops carry a net induced charge into the container below. But this charge is communicated by means of the wire to the ring encircling the right-hand stream. Hence positive charges are induced on this stream as images of the negative charges on the ring. Now we have the mechanism for regenerative feedback because the positive charge on the right

\* L. B. Loeb, *Static Electrification*, Springer, Berlin, 1958, p. 60.

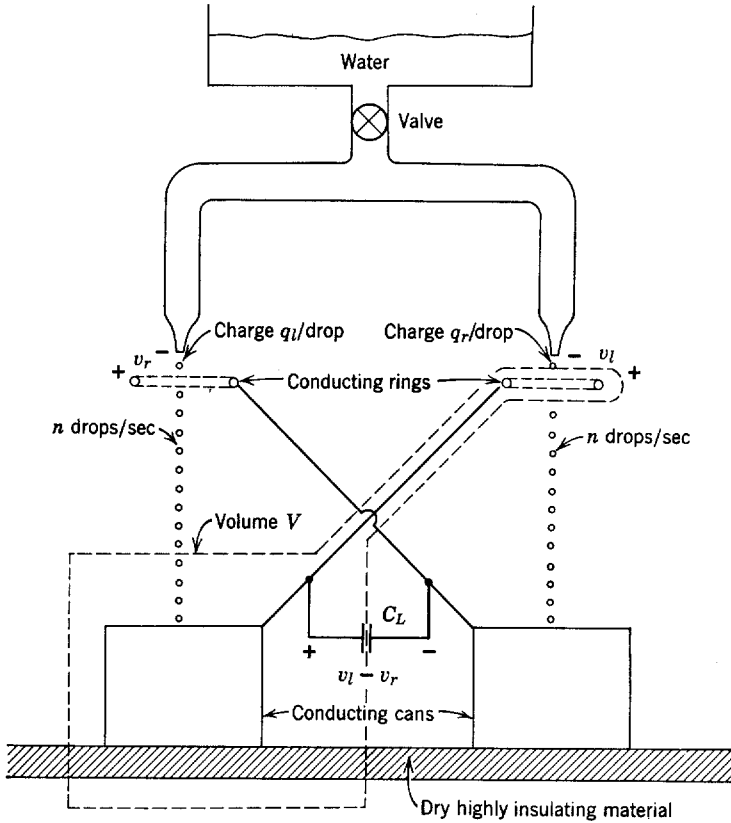


Fig. 7.2.11b Schematic representation of the experiment shown in Fig. 7.2.11a. The capacitance  $C_L$  represents the effect of an external electrostatic voltmeter connected between the cans. The volume  $V$  is used to define quantitatively the voltages  $v_r$  and  $v_l$  in Example 7.2.6.

stream falls into the right container, where it is communicated to the left ring by the connecting wire. On the left ring further negative charges are induced on the stream, with a resulting build up of voltage.

In terms of this explanation it is apparent why it is important that there be two relaxation times in the problem. The charge must relax to the surface of the stream before it breaks up. Once the drops are formed, however, the net charge on an individual drop is essentially conserved. These conditions are satisfied here because the water has a relaxation time that is much shorter than the time required for a drop to form, whereas the air has a relaxation time that is much longer than the time required for a drop to reach the container below.

To model the experiment quantitatively we assume that the charge on each drop is proportional to the voltage on the inducing ring with respect to the water in the pipette (which is at ground potential). Thus

$$q_l = -C_i v_r, \tag{a}$$

$$q_r = -C_i v_l, \tag{b}$$

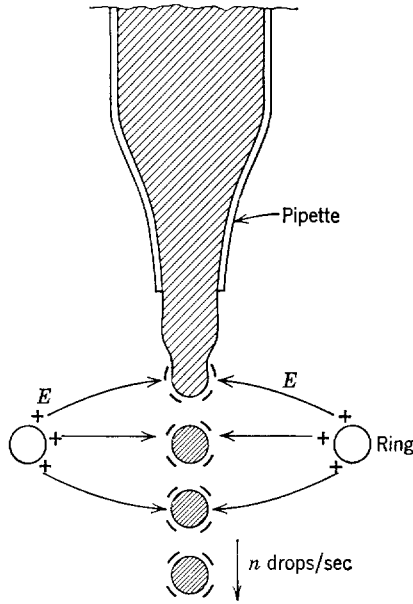


**Fig. 7.2.12** As the drops form near the rings in Fig. 7.2.11, image charges are induced on the surface of the water. When the drops are completely formed (and insulated from one another) they carry a net charge, the sign of which is determined by the sign of the charge on the respective rings.

where  $C_i$  is the constant of proportionality which has the dimension of capacitance. Because there are two equipotentials in addition to ground (the base and the water in the pipettes), the system can be modeled by the equivalent circuit of Fig. 7.2.13. The two current sources represent the rate of charge transport to the cans by the drops. The capacitances  $C$  are capacitances to ground for each can and ring and  $C_L$  is the capacitance between cans plus a load such as an electrostatic voltmeter.

From Fig. 7.2.11b conservation of charge for the volume  $V$  requires

$$-nC_i v_r = C \frac{dv_l}{dt} + C_L \frac{d(v_l - v_r)}{dt} . \tag{c}$$

This is the node equation for the left node in Fig. 7.2.13. Similarly,

$$-nC_i v_l = C \frac{dv_r}{dt} + C_L \frac{d(v_r - v_l)}{dt} . \tag{d}$$

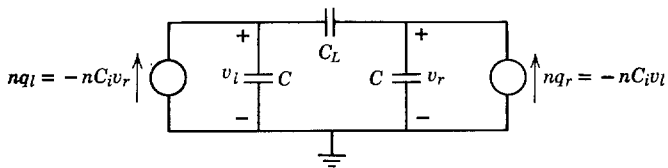


**Fig. 7.2.13** Equivalent circuit of electrostatic generator of Fig. 7.2.11.

These expressions could be reduced to a single second-order equation for either of the dependent variables. Hence there are two solutions. By symmetry we expect that one of these solutions is odd, in the sense that  $v_l = -v_r$ . That this is, in fact, the case can be seen by substituting this condition into (c) and (d) and seeing that they *both* reduce to the form

$$(C + 2C_L) \frac{dv_l}{dt} - nC_l v_l = 0. \quad (e)$$

Similarly, if  $v_r = v_l$ , both (c) and (d) reduce to the form

$$C \frac{dv_l}{dt} + nC_l v_l = 0. \quad (f)$$

The general solutions are appropriate linear combinations of the solutions of (e) and (f):

$$v_l = A \exp\left(\frac{nC_l}{C + 2C_L} t\right) + B \exp\left(-\frac{nC_l}{C} t\right), \quad (g)$$

$$v_r = -A \exp\left(\frac{nC_l}{C + 2C_L} t\right) + B \exp\left(-\frac{nC_l}{C} t\right). \quad (h)$$

where the constants  $A$  and  $B$  are determined by initial conditions. Any slight unbalance in initial voltage (such as that supplied by natural noise) will lead to exponential growth of the odd part of the solution and decay of the even part. In practice the potential difference between the cans builds up until there is electrical breakdown between the cans or the electrical force deflects the drops until they hit the inducing rings. The example discussed here illustrates the effect of material motion on the electric field. The drop deflections represent the reverse effect of the fields on the motion.

### 7.2.3 Sinusoidal Excitation and Charge Relaxation with Motion

A comparison between the developments of Section 7.1, concerned with magnetic diffusion, and those found in this section (Section 7.2) shows a considerable analogy. As might be expected from Section 7.1.3, the introduction of an additional characteristic time by the agent of a sinusoidal excitation makes it possible to tailor the relaxation process to engineering requirements. In this section we undertake to contrast the relaxation process with magnetic diffusion in the presence of motion and with a sinusoidal excitation. The example considered illustrates how charge relaxation can be used to measure the velocity of a moving medium.

A thin slab of slightly conducting material moves to the right with velocity  $V$ , as shown in Fig. 7.2.14. This slab passes between plane parallel electrodes which are broken into three sections with different terminations (Fig. 7.2.14*b*). In the section to the left the plates are driven by a sinusoidally varying potential. From the preceding sections we know that because the slab is insulated from the plates by the intervening air, charges will relax to the surfaces of the slab in a way that tends to exclude the imposed electric field. Hence, as the slab leaves this exciter region at  $z = 0$ , symmetry requires that there be a sinusoidally varying surface charge density  $\sigma_o$  on the upper slab surface and  $-\sigma_o$  on the lower surface.

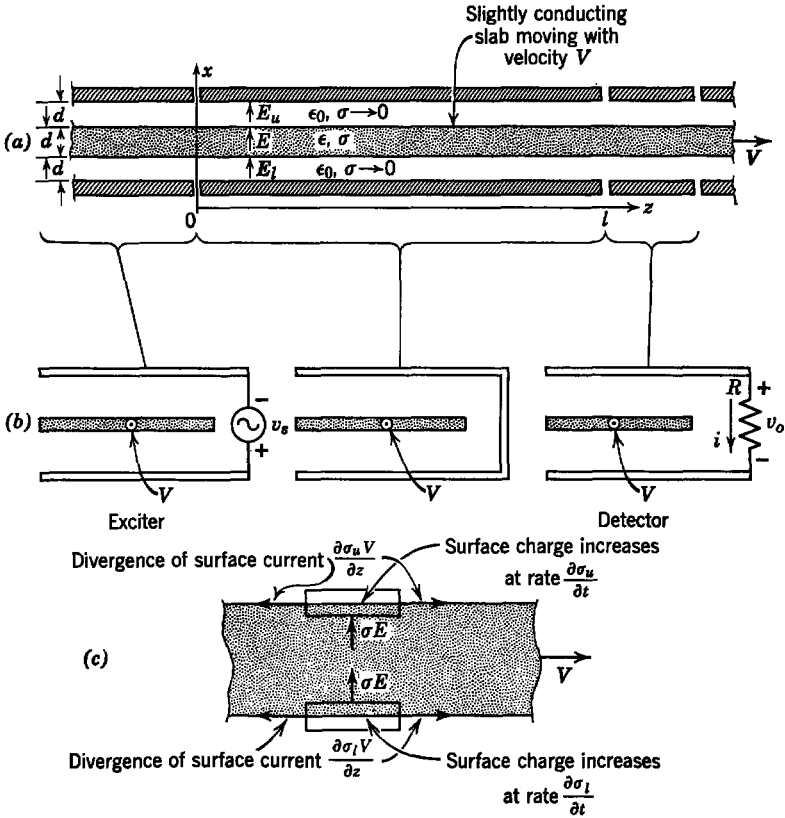


Fig. 7.2.14 (a) A slightly conducting slab moves to the right with velocity  $V$  through electric fields imposed or constrained as shown in (b); (c) conduction currents normal to the surfaces lead to an accumulation of surface charge that can be convected away.

As the slab passes through the region  $0 < z < l$ , the surface charges induced in the exciter region tend to relax so that by the time they reach the detector region to the right the surface charge densities can be considerably attenuated. Those charges that remain induce image charges on the electrodes with a resulting current through the resistance  $R$  and a proportionate generated output signal  $v_o$ . Because of the charge relaxation this signal can be a measure of the material velocity, as shown in the development that follows.

We know from preceding sections that there is no charge in the bulk of the moving slab. On the surfaces, however, the normal conduction current leads to an accumulation of charge that can be convected away by the motion of the slab. Using the electric field intensities defined in Fig. 7.2.14a,

conservation of charge on the upper surface requires that (see Fig. 7.2.14c)

$$\sigma E = \frac{\partial \sigma_u}{\partial t} + V \frac{\partial \sigma_u}{\partial z}, \quad (7.2.18)$$

where the surface charge density  $\sigma_u$  is related to the field intensities by

$$\sigma_u = \epsilon_0 E_u - \epsilon E. \quad (7.2.19)$$

Equation 7.2.18 is a particular application of boundary condition (6.2.36),\* discussed in Section 6.2.2 (see Example 6.2.3).

Similarly, conservation of charge on the lower surface requires

$$-\sigma E = \frac{\partial \sigma_l}{\partial t} + V \frac{\partial \sigma_l}{\partial z}, \quad (7.2.20)$$

where

$$\sigma_l = \epsilon E - \epsilon_0 E_l. \quad (7.2.21)$$

Now, in general, the electric field in the slab, and in the regions above and below, must satisfy the electric field equations with  $\rho_f = 0$ . We can avoid introducing the complication of solving these equations by making a quasi one-dimensional model based on the distance  $d$ , shown in Fig. 7.2.14a, being much smaller than a characteristic (wave) length in the  $z$ -direction. Because the plates are short-circuited in the region  $0 < z < l$ , we not only assume that  $\mathbf{E} = E(z, t)\mathbf{i}_x$  but write

$$d(E_u + E + E_l) = 0 \quad (7.2.22)$$

because the integral of the field along a line joining the plates must be zero.

The one-dimensional model implied by (7.2.18) to (7.2.22) ignores any effect introduced by a component of field intensity in the  $z$ -direction. This component however, does exist and can be computed from  $E_x$  through the condition that the field intensity be irrotational (7.2.1). This second-order effect of one of the field components characterizes "quasi" one-dimensional models as they are found in a variety of physical situations.

At  $z = 0$  we assume that the exciter has induced the surface charges

$$\sigma_l = -\sigma_u = \sigma_o \sin \omega t. \quad (7.2.23)$$

For this reason we look for solutions to (7.2.18) to (7.2.22) that satisfy the requirement that  $E_u = E_l$ . Then, from (7.2.22),

$$E = -(E_u + E_l) = -2E_u, \quad (7.2.24)$$

and it follows from (7.2.19) that the upper surface charge density is related to the field intensity within the moving slab by

$$E = \frac{-2\sigma_u}{\epsilon_0 + 2\epsilon}. \quad (7.2.25)$$

\* See Table 6.1, Appendix E.

This relation, together with (7.2.18) then shows that

$$\frac{\partial \sigma_u}{\partial t} + V \frac{\partial \sigma_u}{\partial z} + \frac{2\sigma}{\epsilon_0 + 2\epsilon} \sigma_u = 0. \tag{7.2.26}$$

Once the upper surface charge density has been found from this expression the lower surface charge density and the three field intensities can be found; That is,  $\sigma_u = -\sigma_l$  (for the excitation considered here),  $E_u = E_l$ , and  $E$  is given by (7.2.24).

Because the charge is varying sinusoidally at  $z = 0$ , we assume that the steady-state solution has the form

$$\sigma_u = \text{Re} [\hat{\sigma}_u(z)e^{j\omega t}]. \tag{7.2.27}$$

Substitution into (7.2.26) shows that

$$\frac{d\hat{\sigma}_u}{dz} + \hat{\sigma}_u \left[ \frac{2\sigma}{(\epsilon_0 + 2\epsilon)V} + \frac{j\omega}{V} \right] = 0. \tag{7.2.28}$$

The solution to this equation, which satisfies the boundary condition of (7.2.23), is

$$\sigma(z, t) = \sigma_o \exp \left[ -\frac{2\sigma l}{(\epsilon_0 + 2\epsilon)V l} z \right] \sin \omega \left( t - \frac{z}{V} \right). \tag{7.2.29}$$

The distribution of surface charge on the moving slab, as given by (7.2.29), is sketched in Fig. 7.2.15. The relaxing charge appears as a wave that propagates to the right with the phase velocity  $V$  and with an exponential envelope determined by the electric Reynolds number  $R_e$ , defined in this case as

$$R_e = \frac{(\epsilon_0 + 2\epsilon)V}{2\sigma l}. \tag{7.2.30}$$

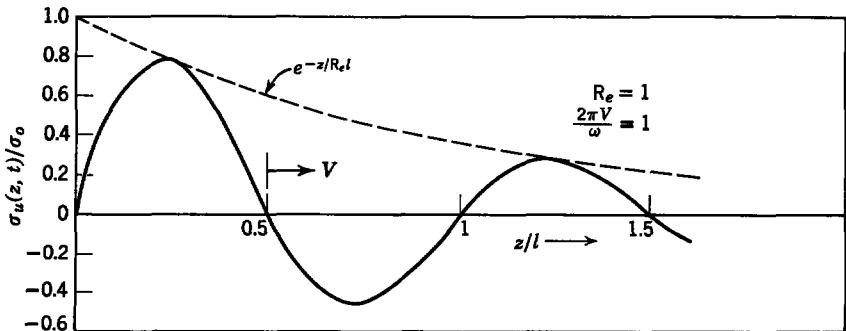


Fig. 7.2.15 Distribution of free charge density on the upper surface of the moving, slightly conducting slab of Fig. 7.2.14. Points of constant phase move with the velocity  $V$  of the material.

Note that by contrast with the magnetic diffusion waves of Section 7.1.3 the relaxation wave found here propagates only by virtue of the material motion. There are no waves that propagate upstream, as there were in Section 7.1.3.

We can make practical use of the relaxation interaction by using the section of plates to the right in Fig. 7.2.14*a, b* to detect the charge on the surface. This is done by attaching a resistance  $R$  between the plates and measuring the induced voltage. If we assume that this resistance is small enough to ensure that the drop in potential across the resistance is negligible compared with  $Ed$  in the section to the left, the induced current is simply

$$i = -A\epsilon_0 \frac{\partial E_x}{\partial t}, \tag{7.2.31}$$

where  $A$  is the area of one of the detector plates. Here we have assumed that the detector plates are of sufficiently small extent in the  $z$ -direction that the integral of the surface charge over the surface of one of the plates can be approximated by the product of  $A$  and the charge at  $z = l$ . It follows that the voltage  $v_o$  from the detector has the magnitude

$$|v_o| = |i| R = \frac{A\epsilon_0\omega\sigma_o}{(\epsilon_0 + 2\epsilon)} e^{-l/R_e}. \tag{7.2.32}$$

The dependence of this signal on the electric Reynolds number is shown in Fig. 7.2.16. As we expected intuitively, the output signal increases with velocity and decreases with conductivity or length  $l$ . Unfortunately, the functional dependence is not so convenient as it was in the system discussed

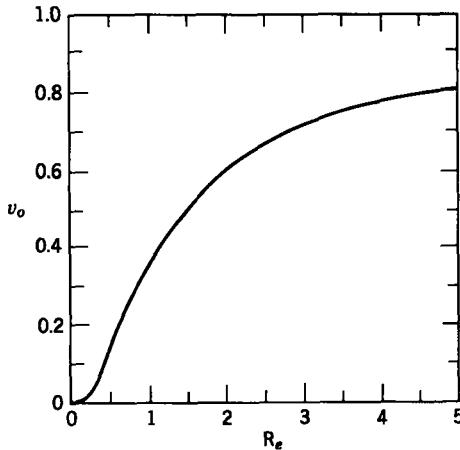


**Fig. 7.2.16** Output voltage as a function of electric Reynolds number  $R_e = [(\epsilon_0 + 2\epsilon)V]/2\sigma l$  for the system of Fig. 7.2.14.

in Section 7.1.3. It is important in this regard to note that systems in which  $R_m$  (magnetic Reynolds number) is on the order of unity and in which  $R_e$  is about unity are in entirely different velocity and conductivity ranges. This point is emphasized in Section 7.3.

#### 7.2.4 Traveling-Wave Charge Relaxation in a Moving Conductor

As illustrated in Section 7.1.4, interactions between a periodic traveling wave and moving media provide considerable physical insight into a diversity of situations. In plane geometry the analytical difficulties involved in magnetic field systems were minimal and in the electric field system considered here the mathematical description is even simpler. Even so, as discussed in Section 7.3, a great deal can be learned that is applicable to more complicated situations.

The physical situation to be considered, which is analogous to that discussed in Section 7.1.4, is shown in Fig. 7.2.17. A slightly conducting material moves to the right with a velocity  $V$  just below a segmented electrode which supports a traveling wave of potential

$$v = \text{Re } \hat{v} e^{j(\omega t - kz)} \quad (7.2.33)$$

It is assumed that material (a) has negligible electrical conductivity. We wish to determine the effect of the motion on the distribution of potential (hence electric field) above and below the surface (at  $x = 0$ ) of the moving conductor. We know in advance that because electrical conductivity  $\sigma$  is uniform in the moving conductor there is no bulk free charge there. Therefore the interactions between the fields and the media occur at the surface of the moving material where surface charges assume a distribution and magnitude determined by the motion and by the velocity of the imposed traveling wave of potential.

Because there is no free charge in either region (a) or (b), (7.2.8), which follows from (7.2.5), reduces to

$$\nabla^2 \phi = \frac{\partial^2 \phi}{\partial x^2} + \frac{\partial^2 \phi}{\partial z^2} = 0. \quad (7.2.34)$$

Here we assume that the problem is two-dimensional so that  $\partial \phi / \partial y = 0$ . The traveling wave of potential given by (7.2.33) constitutes a boundary condition on the potential  $\phi$  in the region (a) above the conductor. To match this condition we assume that the potential  $\phi$  takes the form

$$\phi = \text{Re } \hat{\phi}(x) e^{j(\omega t - kz)} \quad (7.2.35)$$

in both regions (a) and (b). Substitution of this form into (7.2.34) shows that in region (a)

$$\hat{\phi}_a = A \sinh kx + B \cosh kx, \quad (7.2.36)$$

where  $A$  and  $B$  are arbitrary constants to be determined by the boundary

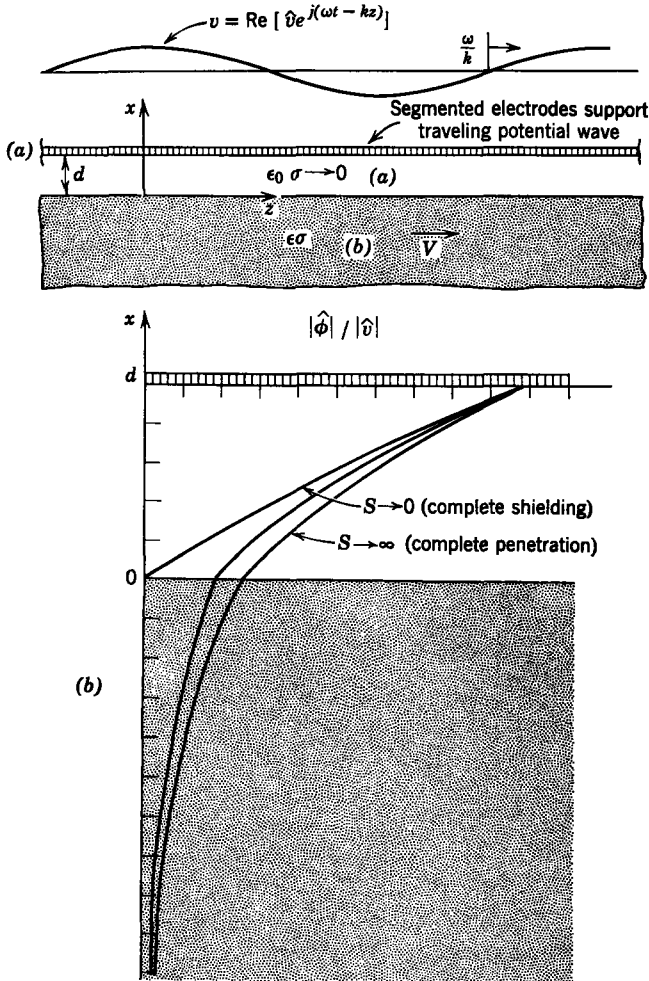


Fig. 7.2.17 (a) A slightly conducting material moves to the right with velocity  $V$  just below a segmented electrode which supports a traveling potential wave; (b) distribution of potential above and below the conductor for various values of  $S = (\omega - kV)\epsilon_0/\sigma$ .

conditions. In region (b) it is more convenient to write the two solutions in the form of exponentials. Then, if we assume that the material in region (b) extends many wavelengths  $2\pi/k$  in the  $-x$ -direction, one of these solutions becomes unbounded as  $x \rightarrow -\infty$  and the appropriate solution is

$$\hat{\phi}_b = Ce^{kx}. \tag{7.2.37}$$

In retaining this half of the solution in region (b) we are assuming that  $k$  is a positive number so that the potential will not go to infinity as  $x \rightarrow -\infty$ .

Three boundary conditions, one of which is (7.2.33), determine the constants  $A$ ,  $B$ , and  $C$ . A second condition develops because the potential is continuous at  $x = 0$ .

$$\hat{\phi}_a(0) = \hat{\phi}_b(0). \quad (7.2.38)$$

The third condition requires conservation of charge on the interface. This equation has the same origins as (7.2.18) in Section 7.2.3. It can be written in terms of the potentials by recognizing that the surface charge density is

$$\sigma_f = \epsilon_0 E_x^a - \epsilon E_x^b = -\epsilon_0 \frac{\partial \phi_a}{\partial x} + \epsilon \frac{\partial \phi_b}{\partial x}. \quad (7.2.39)$$

Then the condition that the conduction current normal to the interface lead to an increase in the surface charge measured in a frame moving with the material is written as

$$-\sigma \frac{\partial \phi_b}{\partial x} = \left( \frac{\partial}{\partial t} + V \frac{\partial}{\partial z} \right) \left( -\epsilon_0 \frac{\partial \phi_a}{\partial x} + \epsilon \frac{\partial \phi_b}{\partial x} \right). \quad (7.2.40)$$

This boundary condition is a particular case of (6.2.36) (see Table 6.1)\*. For the assumed traveling-wave solution (7.2.35) it becomes

$$-\sigma \frac{d\hat{\phi}_b}{dx} = j(\omega - kV) \left( -\epsilon_0 \frac{d\hat{\phi}_a}{dx} + \epsilon \frac{d\hat{\phi}_b}{dx} \right). \quad (7.2.41)$$

Now we are in a position to find the constants  $A$ ,  $B$ , and  $C$  by requiring that (7.2.36) and (7.2.37) satisfy the boundary conditions of (7.2.33), (7.2.38), and (7.2.41). Substitution gives

$$A \sinh kd + B \cosh kd = \hat{v}, \quad (7.2.42)$$

$$B - C = 0, \quad (7.2.43)$$

$$A(jS) - C \left( 1 + jS \frac{\epsilon}{\epsilon_0} \right) = 0, \quad (7.2.44)$$

where  $S$  is the normalized frequency (measured in the moving frame of the material) normalized to the relaxation time

$$S = \frac{(\omega - kV)\epsilon_0}{\sigma}. \quad (7.2.45)$$

The constants  $A$ ,  $B$ , and  $C$  follow from (7.2.42) to (7.2.44) with the result that the potential distributions above and below the moving medium are

$$\phi_a = \text{Re} \frac{\hat{v}}{\Delta} \left[ \left( 1 + jS \frac{\epsilon}{\epsilon_0} \right) \sinh kx + jS \cosh kx \right] e^{j(\omega t - kz)}, \quad (7.2.46)$$

$$\phi_b = \text{Re} \frac{\hat{v}}{\Delta} jS e^{kx} e^{j(\omega t - kz)}, \quad (7.2.47)$$

where  $\Delta = [1 + jS(\epsilon/\epsilon_0)] \sinh kd + jS \cosh kd$ .

\* Appendix E.

The magnitude of the potential distribution predicted by these equations is shown in Fig. 7.2.17*b*. The potentials for an intermediate value and an extreme value of  $S$  are shown to emphasize two important points. When the frequency in the moving frame of the medium is small compared with the reciprocal relaxation time  $S \ll 1$ , the fields are excluded from the material and confined to region (*a*). In this extreme charges have a sufficient amount of time [one period  $2\pi/(\omega - kV)$ , as measured in the frame of the medium] to relax to the surface, where they shield the electric field from the medium; that is, in the limit  $S \rightarrow 0$  the potential in the medium is zero, whereas that just above is

$$\phi_a = \text{Re} \left[ \hat{v} \frac{\sinh kx}{\sinh kd} e^{j(\omega t - kz)} \right]. \quad (7.2.48)$$

Note that this is simply the potential distribution found when the medium is modeled as a perfectly conducting material.

In the opposite extreme, in which the normalized frequency  $|S|$  is very large, the potential distributions become

$$\phi_a = \text{Re} \left[ \hat{v} \frac{\cosh kx + \epsilon/\epsilon_0 \sinh kx}{\cosh kd + \epsilon/\epsilon_0 \sinh kd} e^{j(\omega t - kz)} \right], \quad (7.2.49)$$

$$\phi_b = \text{Re} \left[ \hat{v} \frac{e^{kx} e^{j(\omega t - kz)}}{\cosh kd + \epsilon/\epsilon_0 \sinh kd} \right]. \quad (7.2.50)$$

From Fig. 7.2.17*b* it is clear that in this limit the electric field completely penetrates the moving medium; that is, the potential distribution is just as it would be if the moving medium were modeled as a perfectly insulating material with no free charge at the surface. (Note that (7.2.49) and (7.2.50) show that there is no free charge at  $x = 0$ .) In the high-frequency limit one period of excitation (measured in the moving frame of the medium) is not sufficient time for appreciable free charge to relax to the surface. The parameter  $S$  can be large either because  $\omega$  is large or because  $kV$  is large; that is, if the material is fixed ( $V = 0$ ) and the imposed wave has a high frequency  $\omega$ , the fields penetrate the medium with little shielding from free surface charges. Similarly, the frequency  $\omega$  of the imposed spacially periodic wave could be zero and the same penetration would result by having the material move with a velocity  $V$  large enough that the frequency  $kV$  observed in the moving medium would be large compared with a reciprocal relaxation time.

Although we do not pursue this point here, the traveling wave of potential results in a time average electric shear on the material surface, hence gives rise to a  $z$ -directed force, much as described in Section 7.1.4 for a magnetic field system.\*

\* For a development of this subject see J. R. Melcher, "Traveling-Wave Induced Electroconvection," *Phys. Fluids* **9**, 1548-1555 (1966).

### 7.3 CONCLUSION

The subjects of magnetic diffusion and charge relaxation concern themselves with the behavior of fields in the presence of dissipative media. In each case a characteristic time is associated with the dissipation mechanism. In the case in which currents (hence magnetic fields) diffuse in a conducting medium this is the magnetic diffusion time  $\mu\sigma l^2$ . Similarly, the relaxation time  $\epsilon/\sigma$  for free charge governs the dynamical behavior of electric fields in slightly conducting materials.

The nature of the field solutions is determined by the ratio of these times to times that characterize the dynamics of the system; for example, in a magnetic field system excited at the frequency  $\omega$ , field distributions are determined by the magnetic Reynolds number  $\mu\sigma l^2\omega$  (the ratio of diffusion time to the period of excitation). Alternatively, this number can be thought of as the square of the ratio of a characteristic length in the system to the skin depth  $\delta$  (see Section 7.1.3). A second dynamical time is introduced by motion. With a characteristic velocity  $V$  and length  $l$ , a second magnetic Reynolds number  $\mu\sigma V l$  indicates the importance of material motion in determining the distribution of currents. As we saw in Section 7.1.3, there are situations in which the mechanisms of altering the fields represented by these characteristic numbers are present simultaneously.

In an electric field system excitation at the frequency  $\omega$  leads to an electric Reynolds number  $\omega\epsilon/\sigma$ , whereas motion with the velocity  $V$  through a characteristic distance  $l$  has an effect on the electric field determined by  $\epsilon V/\sigma l$ . A simple summary example provides the opportunity to review these effects while contrasting the behavior of magnetic and electric field systems.

A cylinder of material with conductivity  $\sigma$  is placed between

the pole faces of a magnet as shown in Fig. 7.3.1a.

With the cylinder stationary, the initially uniform magnetic field completely penetrates the conducting material, as shown in Fig. 7.3.2a.

a pair of plane parallel electrodes, as shown in Fig. 7.3.1b.

With the cylinder stationary, the electric field is completely shielded from the interior of the conducting material by free charges that relax to the cylindrical surface, as shown in Fig. 7.3.2b.

The effect of material motion on the steady-state fields is demonstrated by considering the consequences of making the conductor rotate. If the cylinder has a radius  $R$  and angular velocity  $\Omega$ , a characteristic velocity is  $\Omega R$ . The

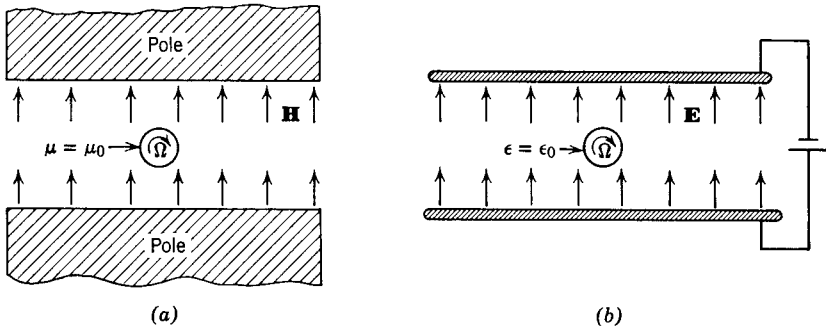


Fig. 7.3.1 (a) Magnetic field system; (b) electric field system.

motion alters the fields of Fig. 7.3.2 if

the magnetic Reynolds number  $R_m$  is significant compared with unity

$$R_m = \mu\sigma VR = \mu\sigma\Omega R^2.$$

the electric Reynolds number  $R_e$  is significant compared with unity

$$R_e = \frac{\epsilon V}{\sigma R} = \frac{\epsilon\Omega}{\sigma}.$$

The conditions under which  $R_m$  and  $R_e$  are on the order of unity are very different; for example, suppose that  $\Omega = 10$  rad/sec and  $R = 10$  cm. Then,

if we let  $\mu = \mu_0$ , the magnetic Reynolds number is unity if  $\sigma = 7.95 \times 10^6$  mhos/m, which is about the conductivity of solder.

if we let  $\epsilon = \epsilon_0$ , the electric Reynolds number is unity if  $\sigma = 8.85 \times 10^{-11}$  mhos/m, which is about the conductivity of corn oil.

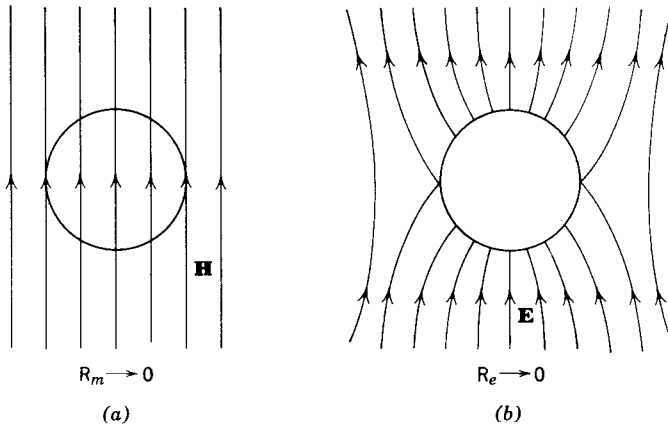


Fig. 7.3.2 (a) Magnetic fields penetrate stationary media; (b) electric fields are excluded from stationary media.

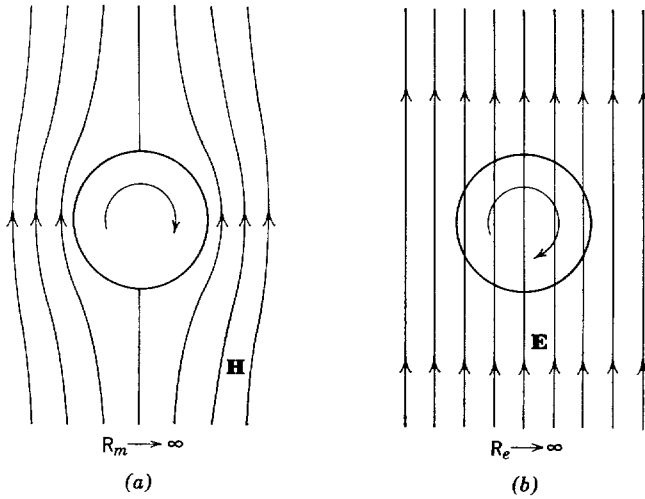


Fig. 7.3.3 (a) Magnetic field completely shielded from cylinder; (b) electric field completely penetrates cylinder.

By making the rotational velocity  $\Omega$  very large there is a large motional effect on the imposed fields. Hence

for  $R_m \gg 1$  the magnetic fields are completely excluded from the rotating cylinder by induced currents, as shown in Fig. 7.3.3a.

for  $R_e \gg 1$  the electric field completely penetrates the rotating cylinder because charges are not able to relax to the cylindrical surface, as shown in Fig. 7.3.3b.

The observations that concern the effect of the rotating cylinders on the fields are evident from Sections 7.1.4 and 7.2.4. There we analyzed (a limiting case in which  $\omega = 0$ ) the field effects of material motion in the presence of a temporally constant, spacially periodic wave. The cylinders considered in this summary are simply those problems with one wavelength along the cartesian coordinate  $z$  “wrapped around on itself.” Of course, the cylindrical geometry requires alterations in the mathematical details. The essential physical features of the problems in cartesian coordinates and those described here, however, are the same.

It should be apparent from the discussions of Sections 7.1.4 and 7.2.4 that we have also developed a picture of what would happen if the cylinders were to be fixed but the fields were to rotate. In the magnetic field case currents would be induced in the rotating cylinder which in turn would develop a torque. This is illustrated in Section 7.1.4 in plane geometry and is a distributed picture of the induction machine discussed in Section 4.1.6b. Situations in which a torque is produced by a rotating electric field are not so common but still exist.